Micro- and Nano- Tomography of Biological Tissues

Marco Stampanoni and Kevin Mader

Swiss Light Source, Paul Scherrer Institut
Institute for Biomedical Engineering, University and ETH Zürich

ETH-227-0965-00 L

Contacts

Prof. Dr. Marco Stampanoni
Institute for Biomedical Engineering
ETH Zürich, ETZ F 85
Gloriastrasse 35
CH-8092 Zürich
Tel: +41 44 632 86 50
+41 56 310 47 24 (PSI)
Email: stampanoni@biomed.ee.ethz.ch

Dr. Kevin Mader
Paul Scherrer Institute
WBBA/213
5232 Villigen

Tel: +41 56 310 5853
Email: kevin.mader@psi.ch

Assistant - Exercises

Mr Ioannis Vogiatzis-Oikonomidis
Swiss Light Source, WBBA/207, 5232 Villigen-PSI
IBT, ETZ H75 , Gloriastrasse 35, 8092 Zürich

Tel: +41 56 310 36 47 (at PSI)
Tel: +41 44 632 52 43 (28 31 or 82 39) (at ETH)
Email: ioannis.vogiatzis@psi.ch

Filippo Arcadu

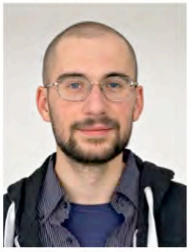

Maria Büchner

Course logistic

Date	Topic	Lecturer	Room
14.09	Lectures Start HS 2015		
21.09	**L: X-ray physics: generation, interactions with matter** E: Papers distribution	Stampanoni	ETZ-E9
28.09	**L: Image formation: from 2D to 3D** E: Exe 1-2	Stampanoni Vogiatzis	ETZ-E9
05.10	**P : Practical "Reconstruction"**	Arcadu/Büchner Vogiatzis	TbD
12.10	**L: Synchrotron light: imaging at the micron scale** E : Exe 3-4	Stampanoni Vogiatzis	ETZ-E9
19.10	**L : Imaging beamlines, in-situ experiments** E : Exe 5-6	Stampanoni Vogiatzis	ETZ-E9
26.10	**L: Visualizing soft tissue: X-ray phase contrast** E: Exe 7-8	Stampanoni Vogiatzis	ETZ-E9
02.11	**P: Practical "Quantification"**	Arcadu/Büchner Vogiatzis	TbD
9.11.	**L: Pushing the limits : Microimaging** E: Exe 9-10	Stampanoni Vogiatzis	ETZ-E9
16.11	**L: Pushing the limits: Nanoimaging** E: Exe 11-12	Stampanoni Vogiatzis	ETZ-E9
23.11	**L: Preprocessing: from measurements to images** E: Student presentation 10min per pair (if needed)	Mader Stampanoni/Mader	ETZ-E9
30.11	**L: Segmentation: from images to features** E: Student presentation 10min per pair	Mader Stampanoni/Mader	ETZ-E9
7.12	**L: Segmentation: from features to statistics** E: Student presentation 10min per pair	Mader Stampanoni/Mader	ETZ-E9
14.12	**E: Visit @ Swiss Light Source**	Stampanoni	SLS (!)

Documents will be put online (polybox) at latest the day before the lecture as PDF
Download at: you will get an email with details (via myStudies)

Course contents

- **Basics of X-ray imaging**
  - X-ray generation and interaction with matter
  - Projection and tomographic imaging, image reconstruction
  - Image quality, noise and dose issues.
- **Imaging at the micron scale**
  - Synchrotron light and its properties
  - Imaging beamlines and related instrumentation
  - Sample environments
  - In-situ experiments
- **Soft-tissue imaging - Phase contrast imaging**
  - Crystal interferometry
  - Transport of Intensity
  - Grating interferometry
- **From micro- to nano-tomographic imaging**
  - Full Field Microscopes
  - Fresnel Zone Plates / KB Systems / CR lenses
  - Scanning Transmission X-ray Microscopy
  - Hard X-rays Microscopes vs Water window
  - Realtime imaging
- **Extracting quantitative information from 3D data**
  - Filtering and Segmentation
  - Morphometrical Analysis
  - Statistics
  - Applications to bio-imaging
- **Experiment at the Swiss Light Source**

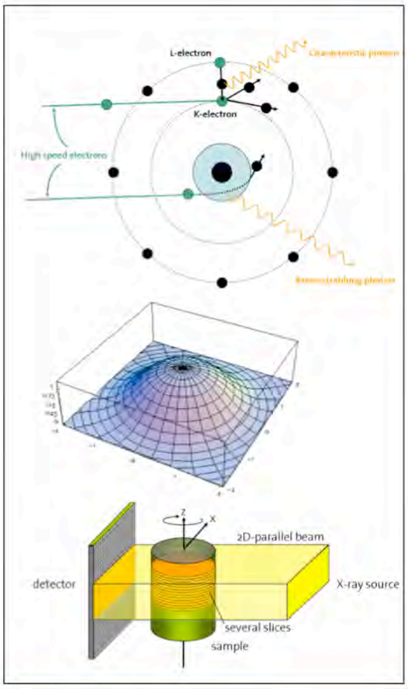

ETH zürich

Course contents

- **Basics of X-ray imaging**
  - X-ray generation and interaction with matter
  - Projection and tomographic imaging, image reconstruction
  - Image quality, noise and dose issues.
- **Imaging at the micron scale**
  - Synchrotron light and its properties
  - Imaging beamlines and related instrumentation
  - Sample environments
  - In-situ experiments
- **Soft-tissue imaging - Phase contrast imaging**
  - Crystal interferometry
  - Transport of Intensity
  - Grating interferometry
- **From micro- to nano-tomographic imaging**
  - Full Field Microscopes
  - Fresnel Zone Plates / KB Systems / CR lenses
  - Scanning Transmission X-ray Microscopy
  - Hard X-rays Microscopes vs Water window
  - Realtime imaging
- **Extracting quantitative information from 3D data**
  - Filtering and Segmentation
  - Morphometrical Analysis
  - Statistics
  - Applications to bio-imaging
- **Experiment at the Swiss Light Source**

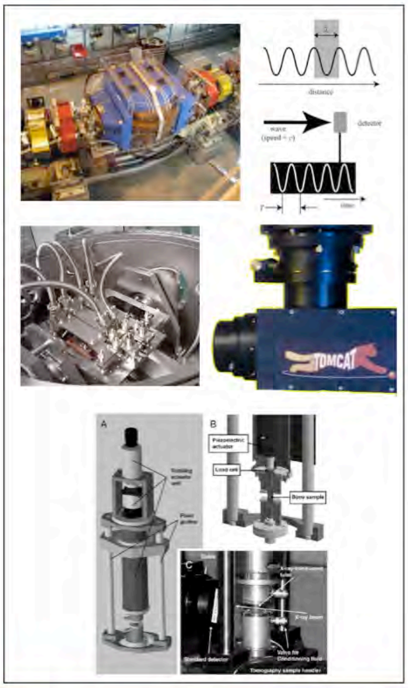

Course contents

- **Basics of X-ray imaging**
  - X-ray generation and interaction with matter
  - Projection and tomographic imaging, image reconstruction
  - Image quality, noise and dose issues.
- **Imaging at the micron scale**
  - Synchrotron light and its properties
  - Imaging beamlines and related instrumentation
  - Sample environments
  - In-situ experiments
- **Soft-tissue imaging - Phase contrast imaging**
  - Crystal interferometry
  - Transport of Intensity
  - Grating interferometry
- **From micro- to nano-tomographic imaging**
  - Full Field Microscopes
  - Fresnel Zone Plates / KB Systems / CR lenses
  - Scanning Transmission X-ray Microscopy
  - Hard X-rays Microscopes vs Water window
  - Realtime imaging
- **Extracting quantitative information from 3D data**
  - Filtering and Segmentation
  - Morphometrical Analysis
  - Statistics
  - Applications to bio-imaging
- **Experiment at the Swiss Light Source**

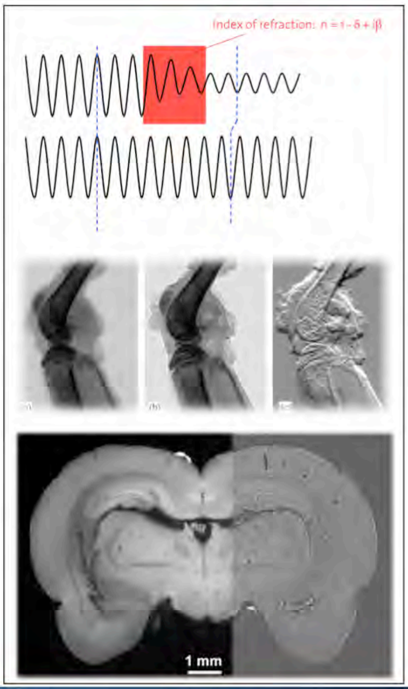

Course contents

- **Basics of X-ray imaging**
  - X-ray generation and interaction with matter
  - Projection and tomographic imaging, image reconstruction
  - Image quality, noise and dose issues.
- **Imaging at the micron scale**
  - Synchrotron light and its properties
  - Imaging beamlines and related instrumentation
  - Sample environments
  - In-situ experiments
- **Soft-tissue imaging - Phase contrast imaging**
  - Crystal interferometry
  - Transport of Intensity
  - Grating interferometry
- **From micro- to nano-tomographic imaging**
  - Full Field Microscopes
  - Fresnel Zone Plates / KB Systems / CR lenses
  - Scanning Transmission X-ray Microscopy
  - Hard X-rays Microscopes vs Water window
  - Realtime imaging
- **Extracting quantitative information from 3D data**
  - Filtering and Segmentation
  - Morphometrical Analysis
  - Statistics
  - Applications to bio-imaging
- **Experiment at the Swiss Light Source**

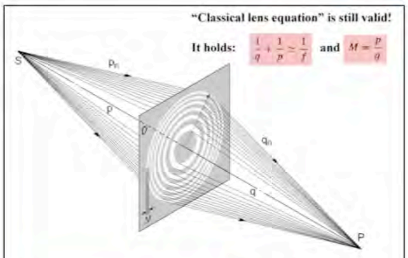

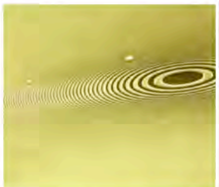

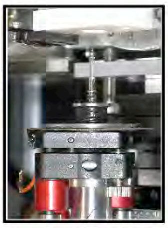

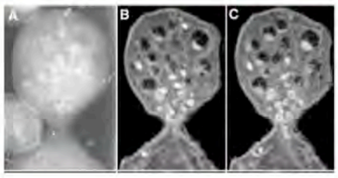

ETH zürich

Course contents

- **Basics of X-ray imaging**
  - X-ray generation and interaction with matter
  - Projection and tomographic imaging, image reconstruction
  - Image quality, noise and dose issues.
- **Imaging at the micron scale**
  - Synchrotron light and its properties
  - Imaging beamlines and related instrumentation
  - Sample environments
  - In-situ experiments
- **Soft-tissue imaging - Phase contrast imaging**
  - Crystal interferometry
  - Transport of Intensity
  - Grating interferometry
- **From micro- to nano-tomographic imaging**
  - Full Field Microscopes
  - Fresnel Zone Plates / KB Systems / CR lenses
  - Scanning Transmission X-ray Microscopy
  - Hard X-rays Microscopes vs Water window
  - Realtime imaging
- **Extracting quantitative information from 3D data**
  - Filtering and Segmentation
  - Morphometrical Analysis
  - Statistics
  - Applications to bio-imaging
- **Experiment at the Swiss Light Source**

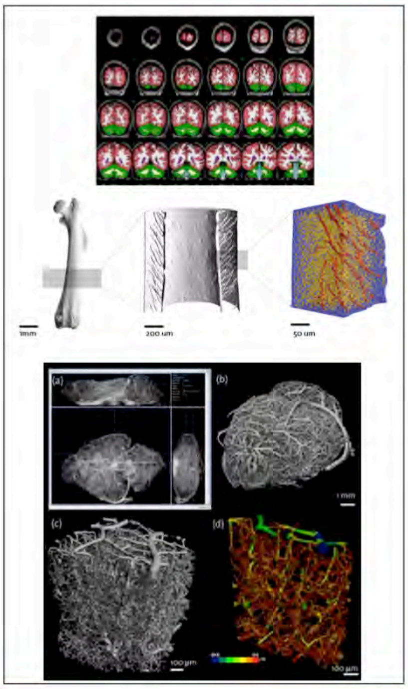

Course contents

- **Basics of X-ray imaging**
  - X-ray generation and interaction with matter
  - Projection and tomographic imaging, image reconstruction
  - Image quality, noise and dose issues.
- **Imaging at the micron scale**
  - Synchrotron light and its properties
  - Imaging beamlines and related instrumentation
  - Sample environments
  - In-situ experiments
- **Soft-tissue imaging - Phase contrast imaging**
  - Crystal interferometry
  - Transport of Intensity
  - Grating interferometry
- **From micro- to nano-tomographic imaging**
  - Full Field Microscopes
  - Fresnel Zone Plates / KB Systems / CR lenses
  - Scanning Transmission X-ray Microscopy
  - Hard X-rays Microscopes vs Water window
  - Realtime imaging
- **Extracting quantitative information from 3D data**
  - Filtering and Segmentation
  - Morphometrical Analysis
  - Statistics
  - Applications to bio-imaging
- **Experiment at the Swiss Light Source**

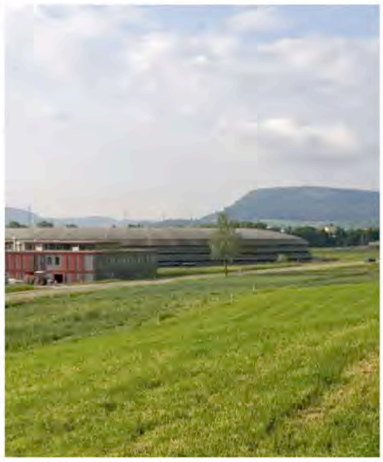

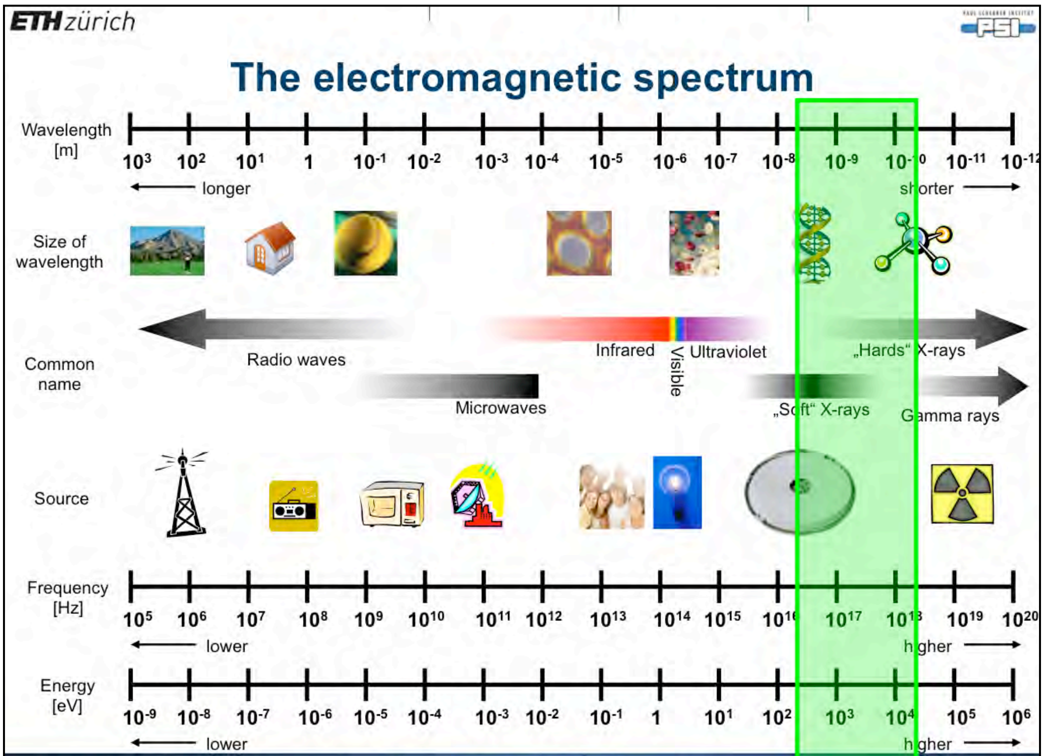
ETH zürich
The electromagnetic spectrum
Wavelength [m]
10^3 10^2 10^1 1 10^-1 10^-2 10^-3 10^-4 10^-5 10^-6 10^-7 10^-8 10^-9 10^-10 10^-11 10^-12
longer
shorter
Size of wavelength
Common name
Radio waves
Microwaves
Infrared
Visible
Ultraviolet
„Soft“ X-rays
„Hards“ X-rays
Gamma rays
Source
Frequency [Hz]
10^5 10^6 10^7 10^8 10^9 10^10 10^11 10^12 10^13 10^14 10^15 10^16 10^17 10^18 10^19 10^20
lower
higher
Energy [eV]
10^-9 10^-8 10^-7 10^-6 10^-5 10^-4 10^-3 10^-2 10^-1 1 10^1 10^2 10^3 10^4 10^5 10^6
lower
higher

What can X-rays tell you ?

Microscopy

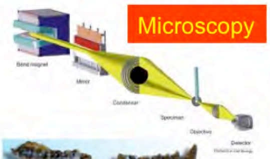

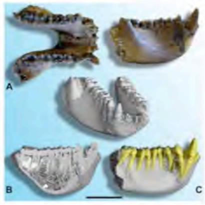

Astronomy

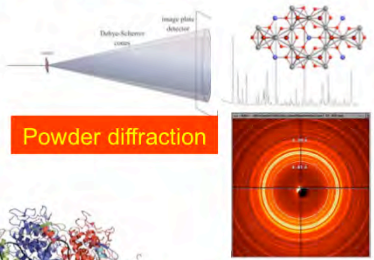

Powder diffraction

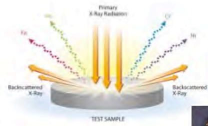

Fluorescence

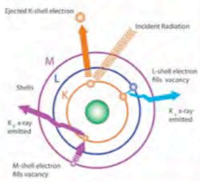

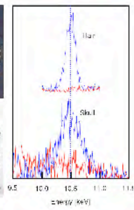

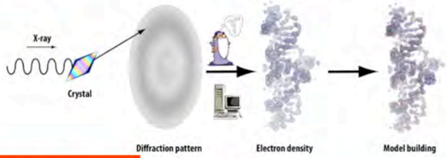

Protein cristallography

A short "nobel" story

W. Röntgen, 1901

M. von Laue, 1914

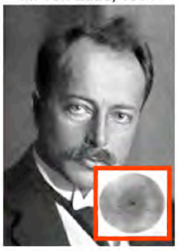

W. H. Bragg, W. L. Bragg, 1915

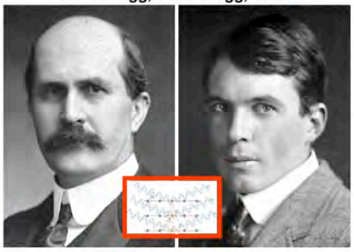

C. Barkla, 1917

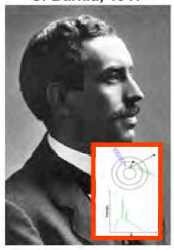

G. Hounsfield, A. Cormack, 1979

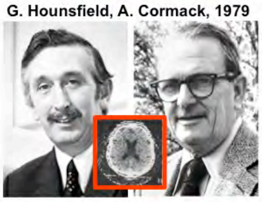

F. Crick, J. Watson, M. Wilkins, 1962

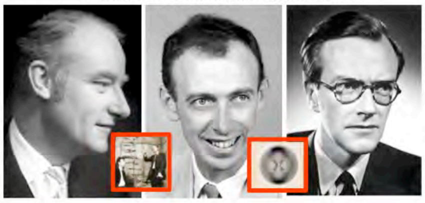

A. Yonath, V. Ramakrishnan, T. Steitz, 2009

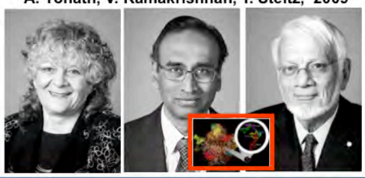

http://www.nobelprize.org

X-ray imaging yesterday…

First X-ray image, 1896

X-ray micro-radiography of a fruit fly

Absorption-based tomographic microscopy

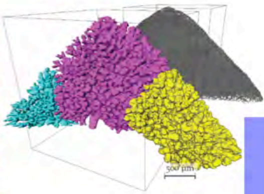

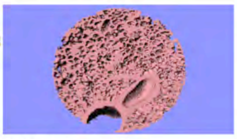

Morphology of lung acini
Haberthür et al., Journal of Synchrotron Radiation, 17(5), 2010
Schittny et al., American Journal of Physiolgy 294 (L246), 2008

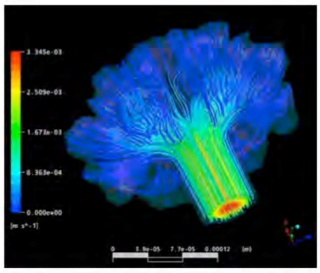

Simulation of blood flow in brain micro-vasculature
Reichold et al., Journal of Cerebral Blood Flow and Metabolism, 29(8), 1429-1443 (2009)

Air-flow simulation in terminal alveoli
Sznitman et al., Journal of Visualization, Online Version, June 2010

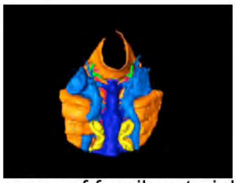

Tomographic microscopy of fossil materials
P. Donoghue et al., Nature 442, Aug. 2006 Z. Gai, Nature 476, Aug. 2011
W. Hagadorn et al., Science 314, Oct. 2006 T. Huldgren, Science 334, Dec. 2011

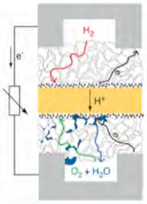

In-situ visualization of operating fuel cell
J. Eller et al., Journal of the Electrochemical Society 158, B963 (2011)

Imaging in 4D

For instance: investigate the biomechanics underlying flight manoeuvres and gaze shifts

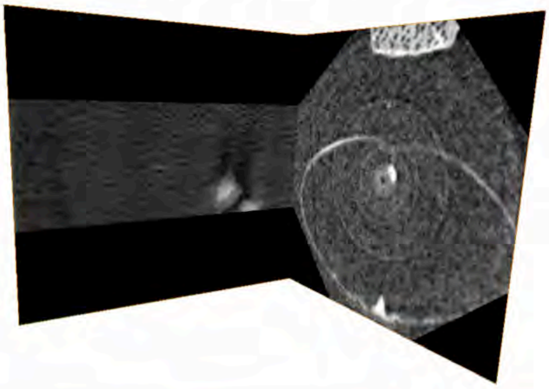

You will learn how to acquire such data and perform such investigations!

Movie courtesy of S. Walker *et al.*, IC, London

Improve contrast from soft tissue

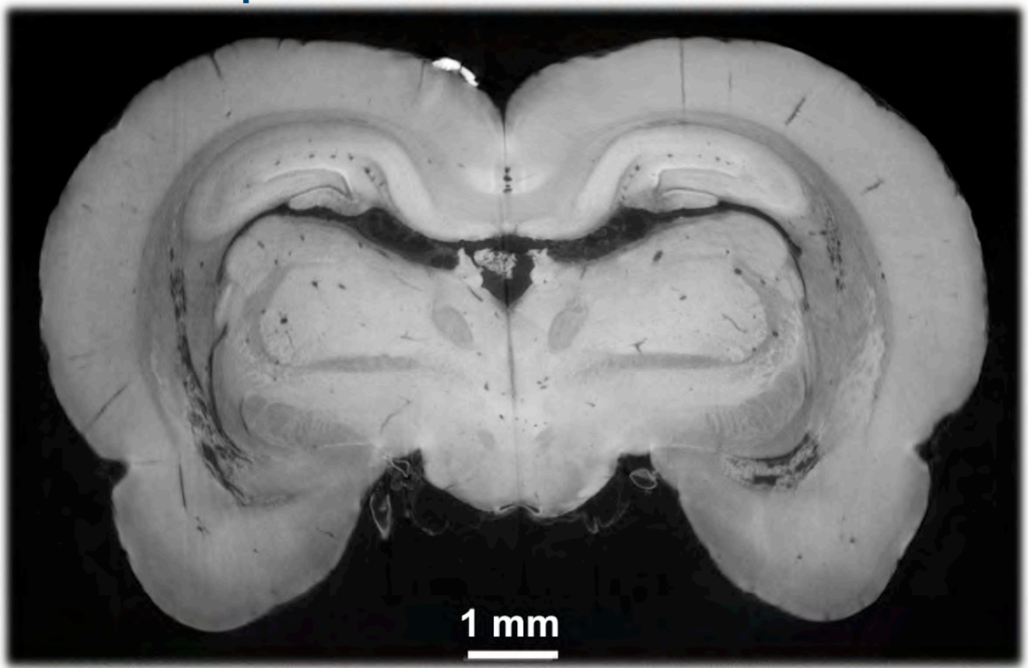

Improve contrast from soft tissue

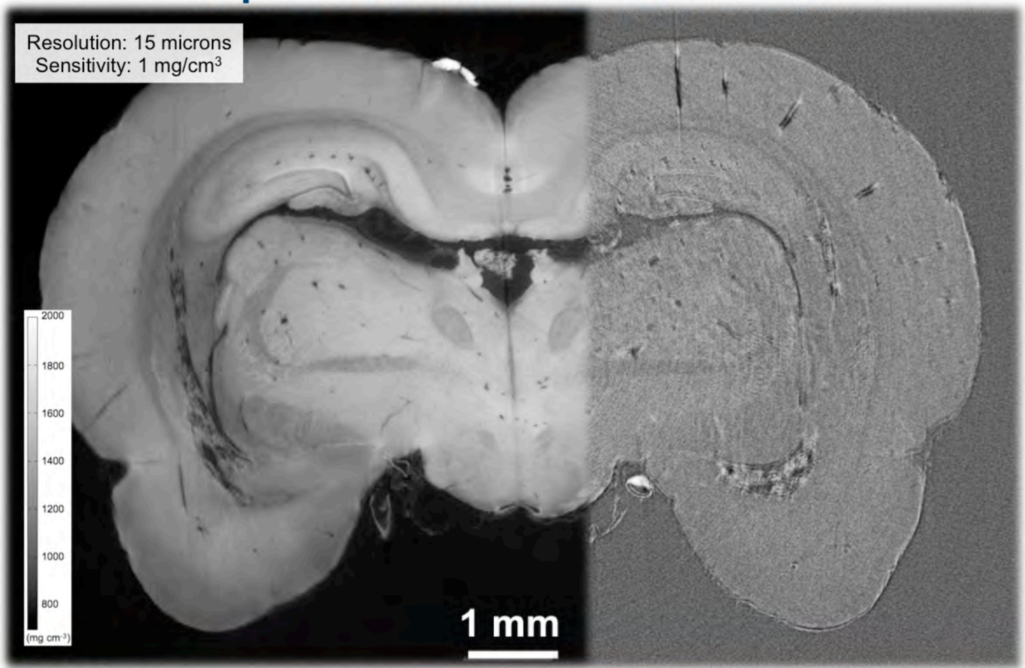

Enhanced *spiculations* visibility

Z. Wang, XNPIG 2012

Enhanced *spiculations* visibility

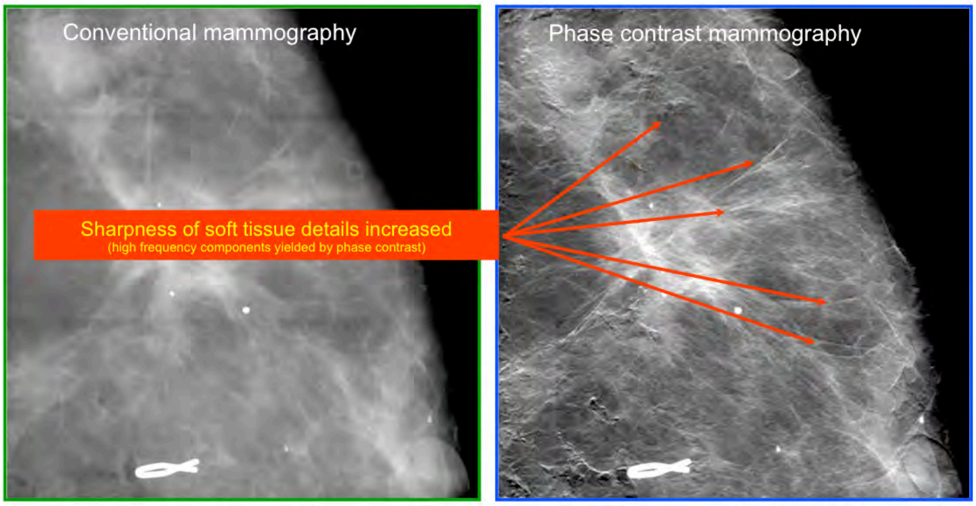

Same dose!

Z. Wang, XNPIG 2012

.

New perspectives for medical imaging

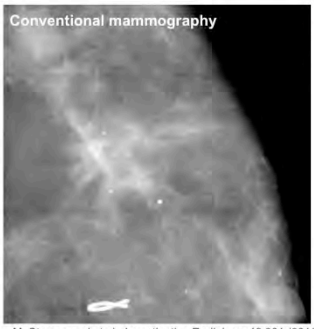

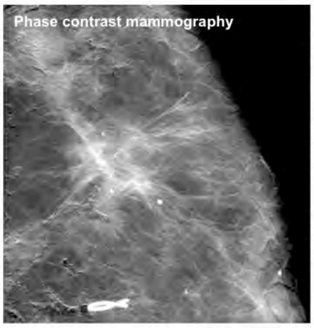

EARLY BREAST CANCER DETECTION (2D)

- Sharper and better lesion delineation
- Sharper microcalcifications
- Non-invasive microcalcification classification
- Improved spiculations identifications
- Improved clinical relevance
- General better image quality

M. Stampanoni et al., Investigative Radiology, 46:801 (2011)
N. Hauser et al., Investigative Radiology 49:3 (2014)
Z. Wang et al., Nat. Communications 5:3797 (2014)

ENHANCED HAND IMAGING (3D)

- Improved soft tissue visibility
  - Tendons and ligaments

T. Donath et al., Investigative Radiology 45:7 (2010)
T. Thüring et al., Skeletal Radiology 42 (2013)

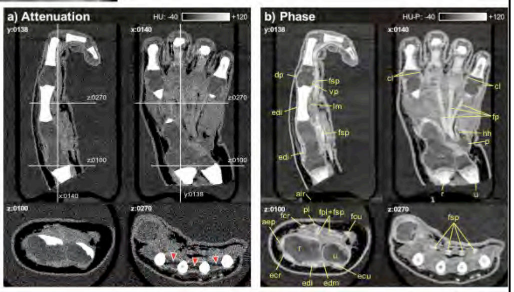

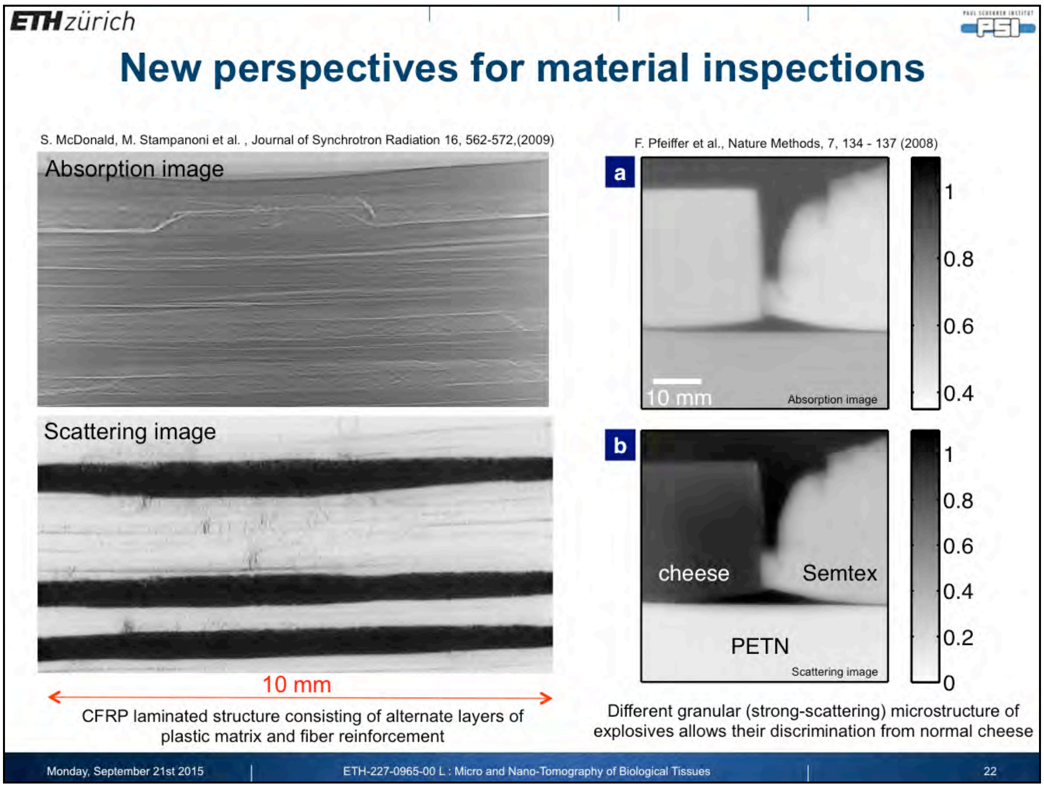

Carbon Fiber Reinforced Polymers…

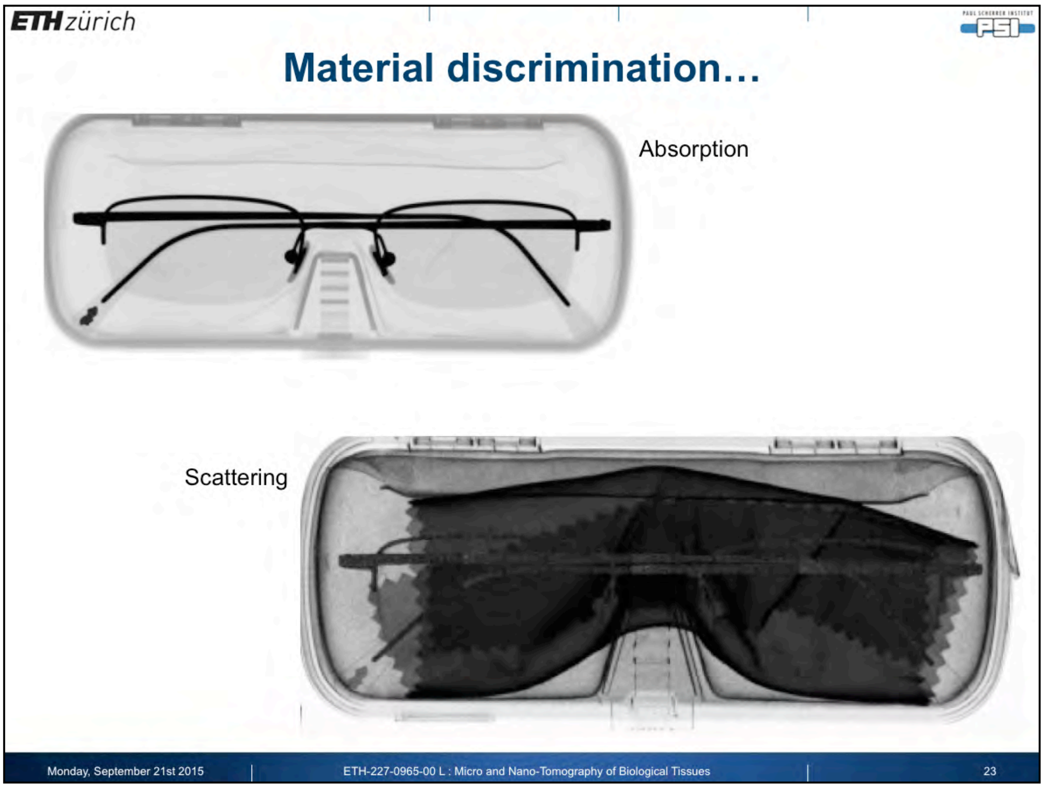

Cleaning flanel…

X-ray sources of the 21st century

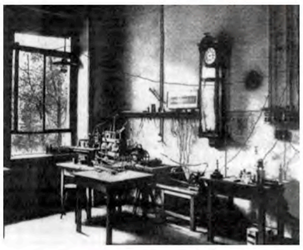

Röntgen's Lab, Late 19th century

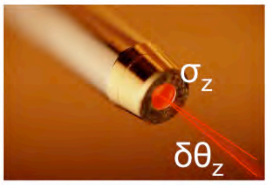

Swiss Light Source, Today

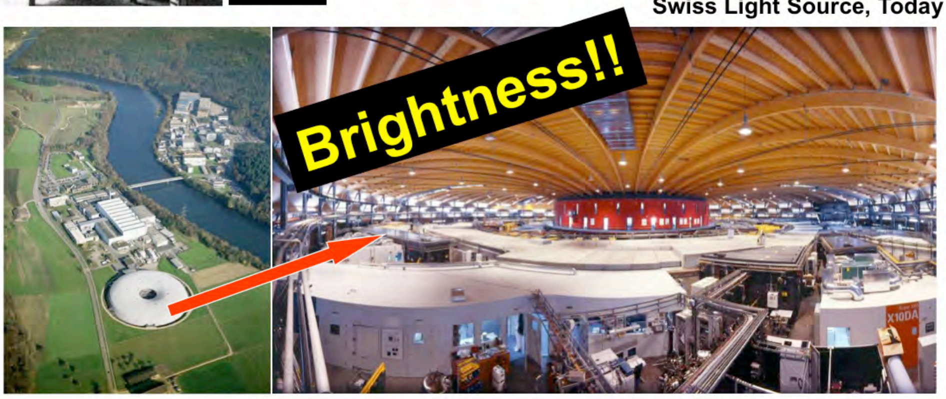

Why a synchrotron for imaging ?

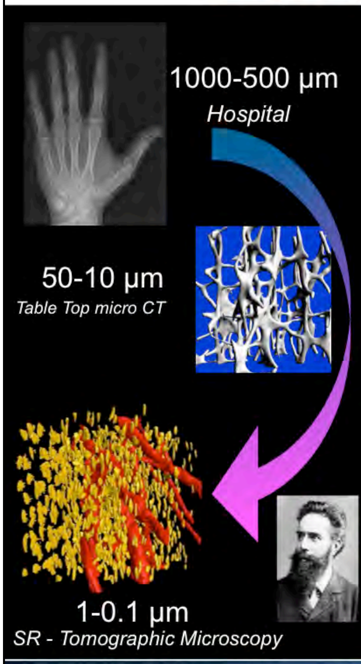

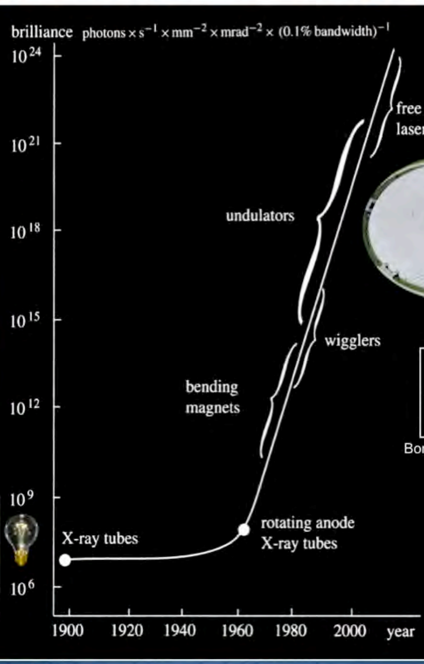

$$\Phi \propto \frac{quality^2}{res^4 \cdot contr^2}$$

Bonse et al., Prog. Biophys. Molec. Biol., Vol. 65, No.1, pp. 133-169, 1996

The Swiss Light Source at the Paul Scherrer Institute

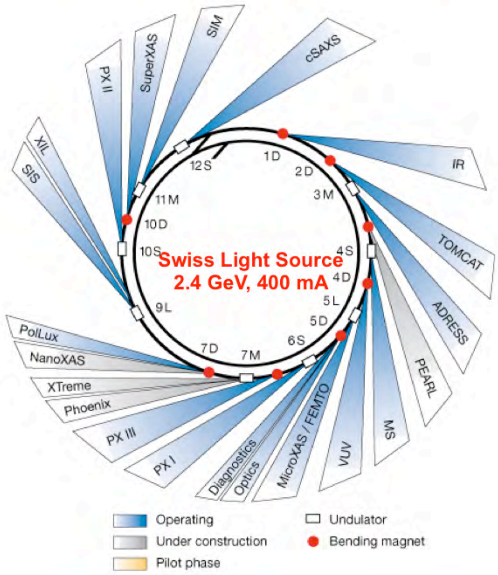

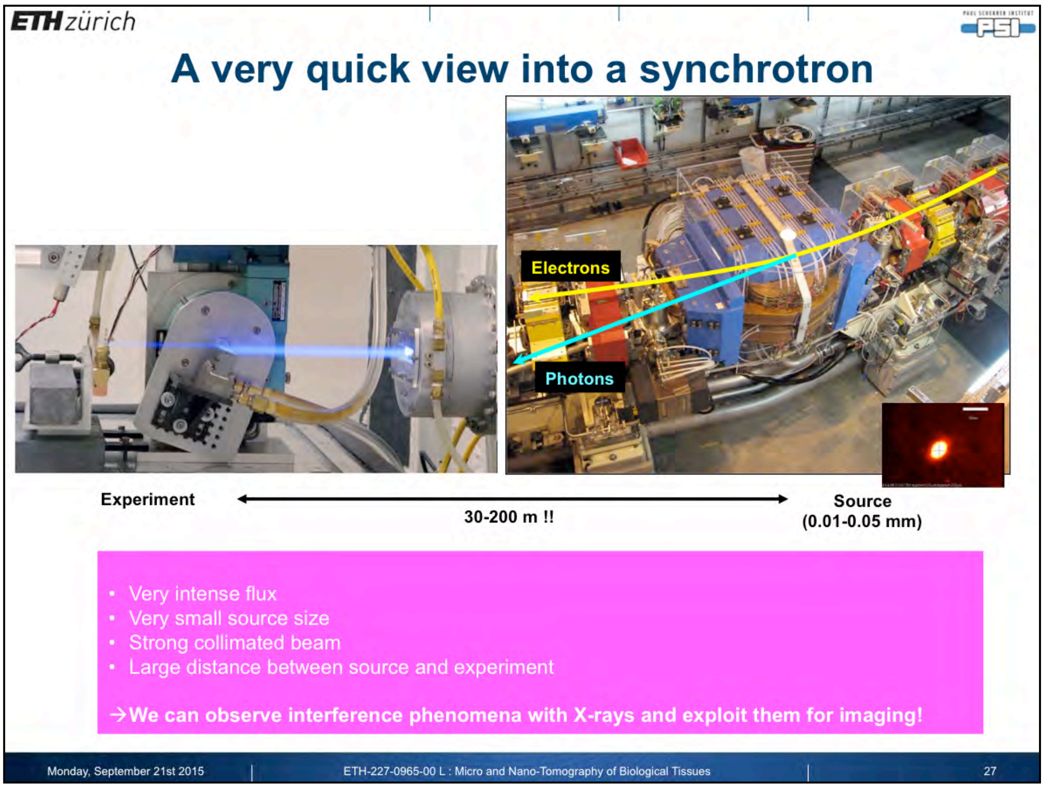

Die blaue Farbe kommt aus der Ionisierung des Sauerstoff in der Luft welche von den sehr starken Röntgenstrahl verursacht…

X-ray sources

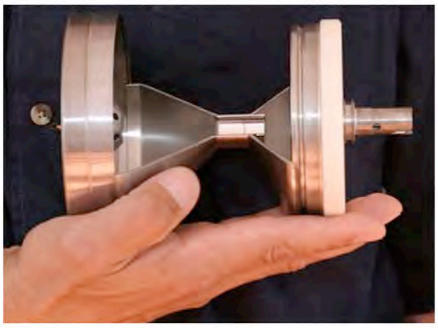

X-ray tubes

- Compact, light source
- Availability, cheap

- Polychromatic
- Low flux
- Highly divergent

Synchrotron radiation

- Monochromatic
- High flux
- Highly collimated
- Polarized

- Large scale facility
- Very expensive

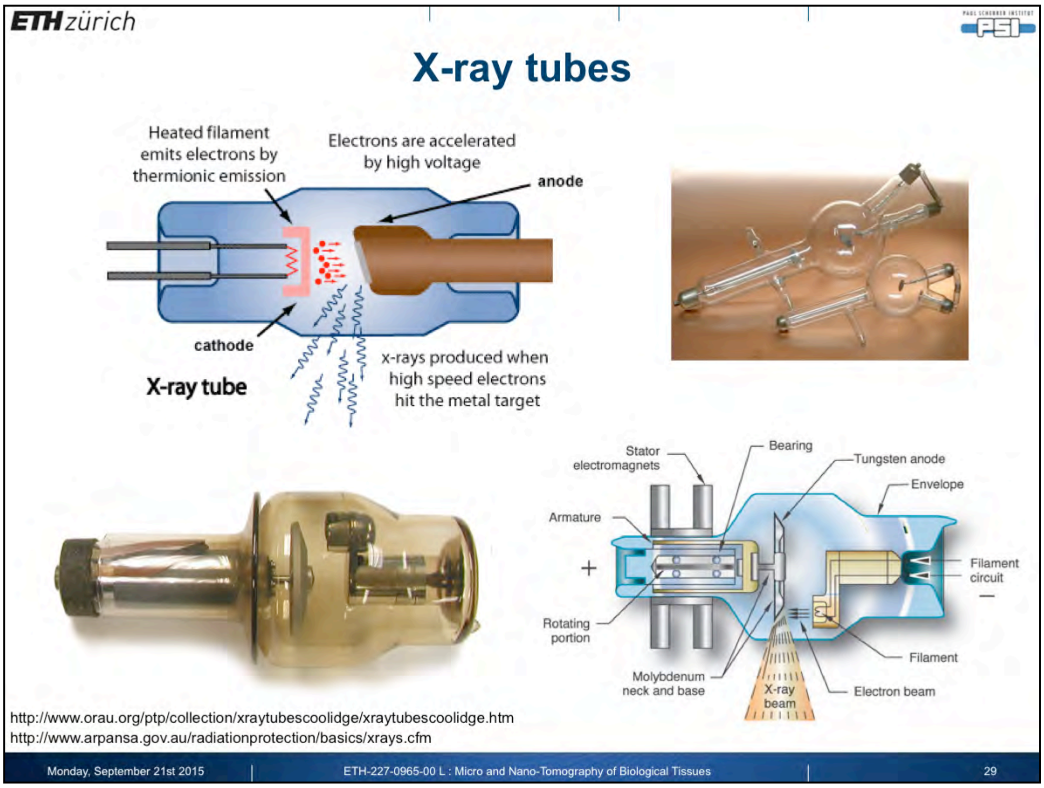

An x-ray tube is an *energy converter*. It receives electrical energy and converts it into two other forms: X-radiation and heat. The heat is an undesirable byproduct. X-ray tubes are designed and constructed to maximize x-ray production and to dissipate heat as rapidly as possible.
The x-ray tube is a relatively simple electrical device typically containing two principle elements: a **cathode** and an **anode**. As the electrical current flows through the tube from cathode to anode, the electrons undergo an energy loss, which results in the generation of x-radiation.

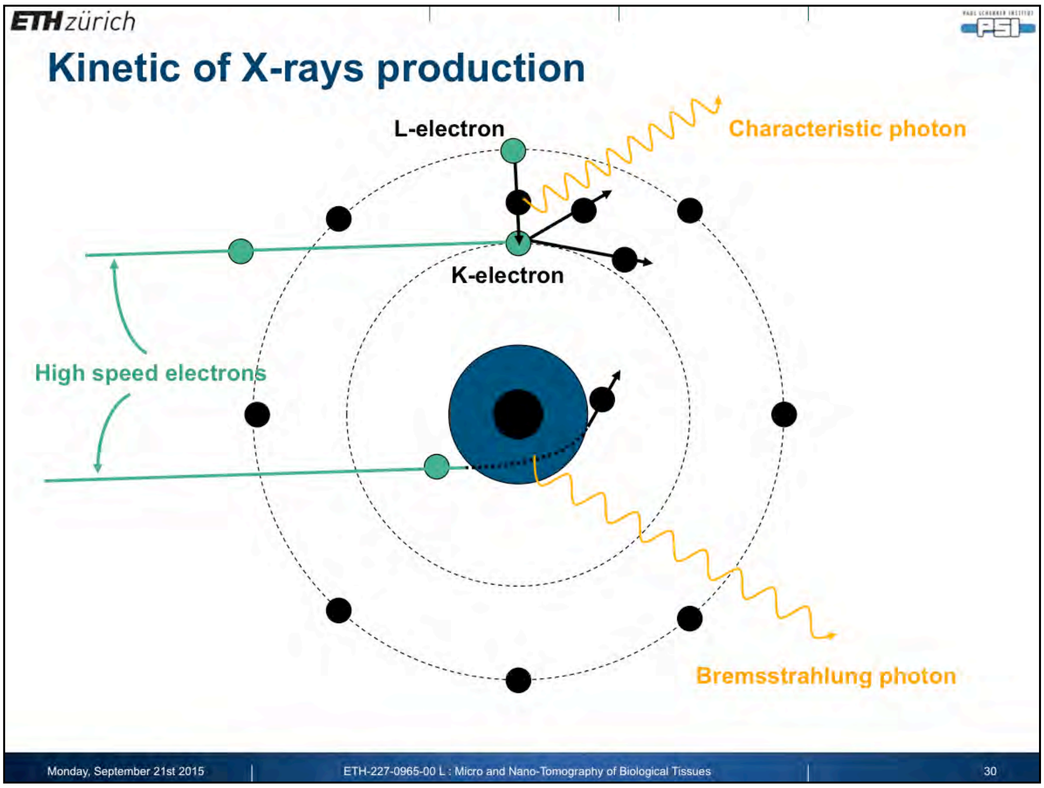

After the electrons are emitted from the cathode, they come under the influence of an electrical force pulling them toward the anode. This force accelerates them, causing an increase in velocity and kinetic energy. This increase in kinetic energy continues as the electrons travel from the cathode to the anode. As the electron moves from cathode to anode, however, its electrical potential energy decreases as it is converted into kinetic energy all along the way. Just as the electron arrives at the surface of the anode its potential energy is lost, and all its energy is kinetic. At this point the electron is traveling with a relatively high velocity determined by its actual energy content. A 100-keV electron reaches the anode surface traveling at more than one half the velocity of light. When the electrons strike the surface of the anode, they are slowed very quickly and lose their kinetic energy; the kinetic energy is converted into either x-radiation or heat.

The electrons interact with individual atoms of the anode material. Two types of interactions produce radiation. An interaction with electron shells produces **characteristic x-ray** photons; interactions with the atomic nucleus produce **Bremsstrahlung x-ray** photons.

X-ray generation: Bremsstrahlung

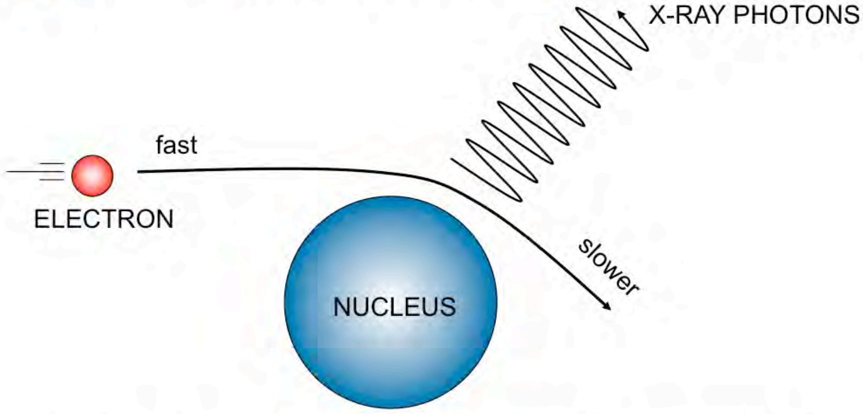

A fast moving electron decelerates when it swings around a heavy nucelus:

- electron interacts with electrons in outer shells
- energy depends in distance at which electrons passes the nuclei
- spectrum continuous until E_{max}
- interaction cross section depends on Z value of nuclei and E of the moving electron

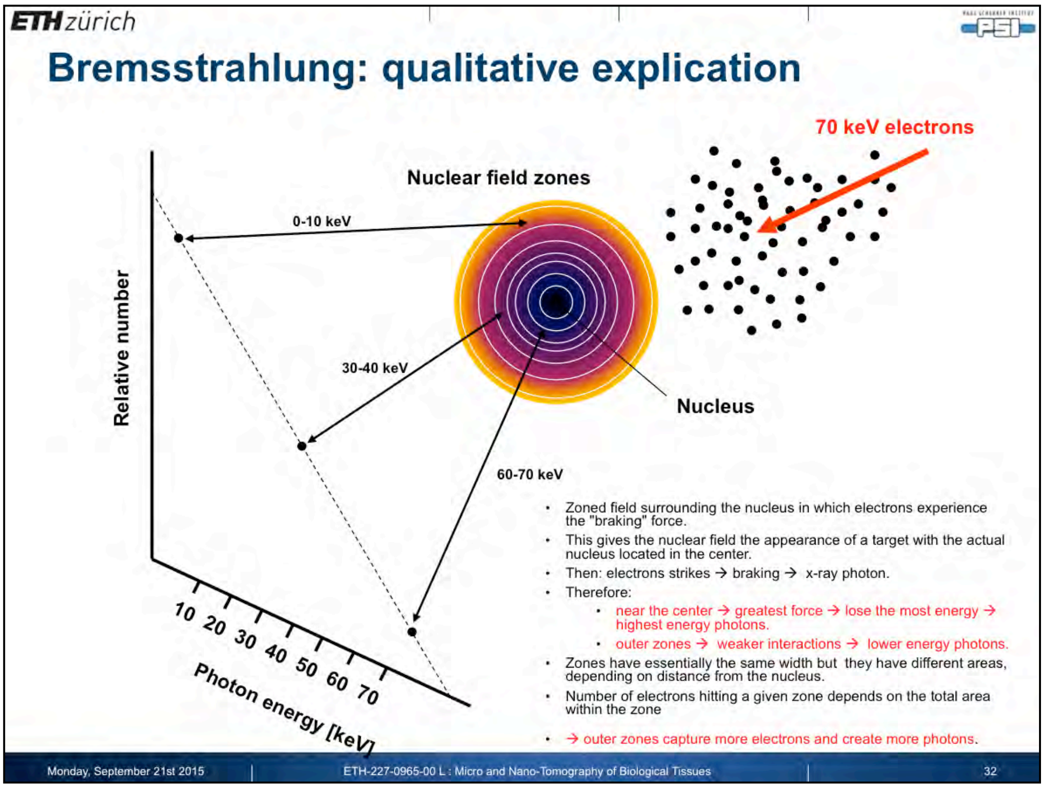

The interaction that produces the most photons is the Bremsstrahlung process. Bremsstrahlung is a German word for "braking radiation" and is a good description of the process. Electrons that penetrate the anode material and pass close to a nucleus are deflected and slowed down by the attractive force from the nucleus. The energy lost by the electron during this encounter appears in the form of an x-ray photon. All electrons do not produce photons of the same energy.

Spectrum Only a few photons that have energies close to that of the electrons are produced; most have lower energies. Although the reason for this is complex, a simplified model of the Bremsstrahlung interaction is shown below. First, assume that there is a space, or field, surrounding the nucleus in which electrons experience the "braking" force. This field can be divided into zones, as illustrated. This gives the nuclear field the appearance of a target with the actual nucleus located in the center. An electron striking anywhere within the target experiences some braking action and produces an x-ray photon. Those electrons striking nearest the center are subjected to the greatest force and, therefore, lose the most energy and produce the highest energy photons. The electrons hitting in the outer zones experience weaker interactions and produce lower energy photons. Although the zones have essentially the same width, they have different areas. The area of a given zone depends on its distance from the nucleus. Since the number of electrons hitting a given zone depends on the total area within the zone, it is obvious that the outer zones capture more electrons and create more photons. From this model, an x-ray energy spectrum, such as the one shown below, could be predicted.

The basic Bremsstrahlung spectrum has a maximum photon energy that corresponds to the energy of the incident electrons. This is 70 keV for the example shown. Below this point, the number of photons produced increases as photon energy decreases. The spectrum of x-rays emerging from the tube generally looks quite different from the one shown here because of selective absorption within the filter.

A significant number of the lower-energy photons are absorbed or filtered out as they attempt to pass through the anode surface, x-ray tube window, or added filter material. X-ray beam filtration is discussed more extensively in a later chapter. The amount of filtration is generally dependent on the composition and thickness of material through which the x-ray beam passes and is generally what determines the shape of the low-energy end of the spectrum curve.

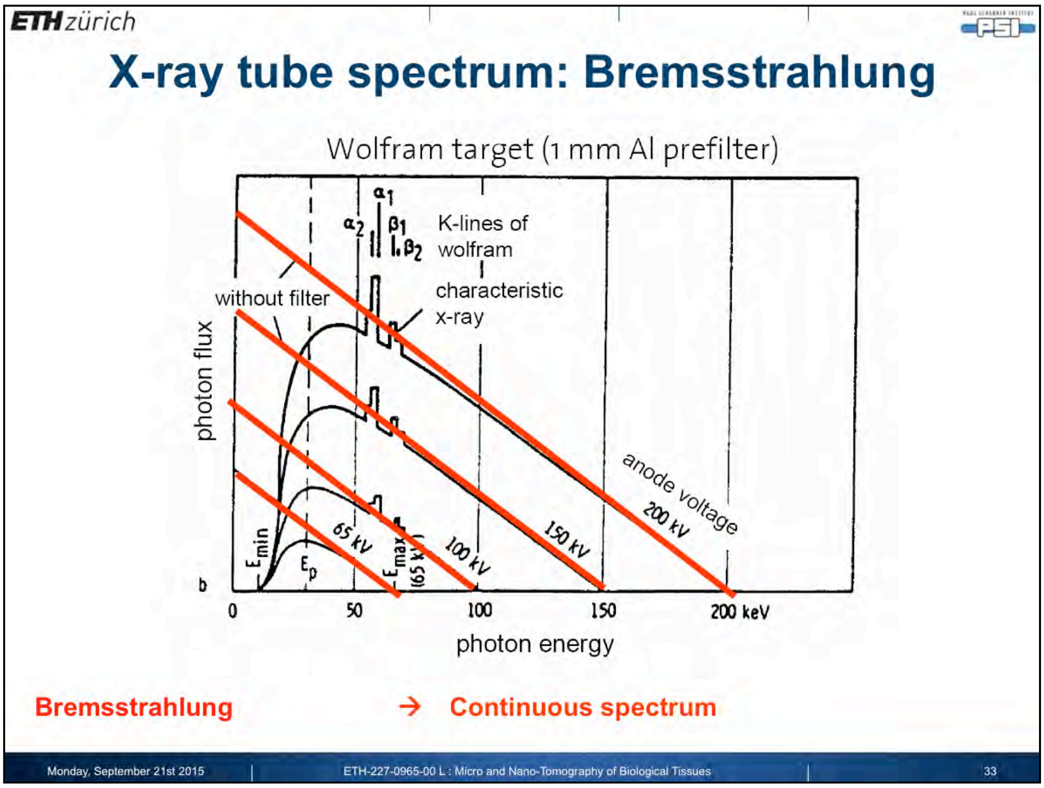

The high-energy end of the spectrum is determined by the KV (kilovoltage) applied to the x-ray tube. This is because the KV establishes the energy of the electrons as they reach the anode, and no x-ray photon can be created with an energy greater than that of the electrons. The maximum photon energy, therefore, in keV is numerically equal to the maximum applied potential in kV (kilovolts). In some x-ray equipment, the voltage applied to the tube might vary during the exposure because of the cycle nature of the AC (alternating current) electrical system. . The maximum photon energy is determined by the maximum, or peak, voltage during the voltage cycle. This value is generally referred to as the kilovolt peak (KVP) and is one of the adjustable factors of x-ray equipment.

In addition to establishing the maximum x-ray photon energy, the KVP has a major role in determining the quantity of radiation produced for a given number of electrons, such as 1 mAs, striking the anode. Since the general efficiency of x-ray production by the Bremsstrahlung process is increased by increasing the energy of the bombarding electrons, and the electronic energy is determined by the KVP, it follows that the KVP affects x-ray production efficiency.

Changing the KVP will generally alter the Bremsstrahlung spectrum. The total area under the spectrum curve represents the number of photons or quantity of radiation produced. If no filtration is present where the spectrum is essentially a triangle, the amount of radiation produced is approximately proportional to the KV squared. With the presence of filtration, however, increasing the KV also increases the relative penetration of the photons, and a smaller percentage is filtered out. This results in an even greater increase in radiation output with KVP

Kinetic of X-rays production

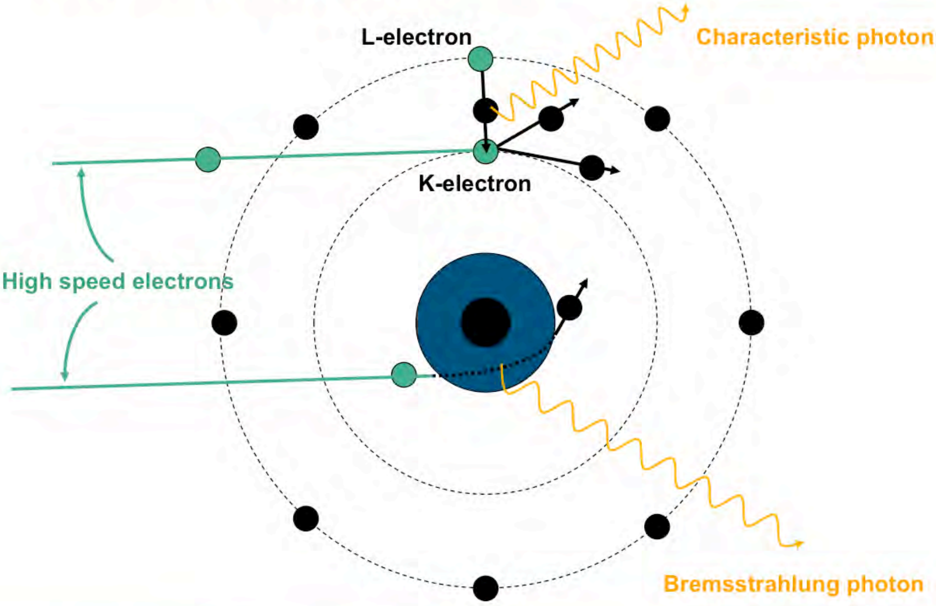

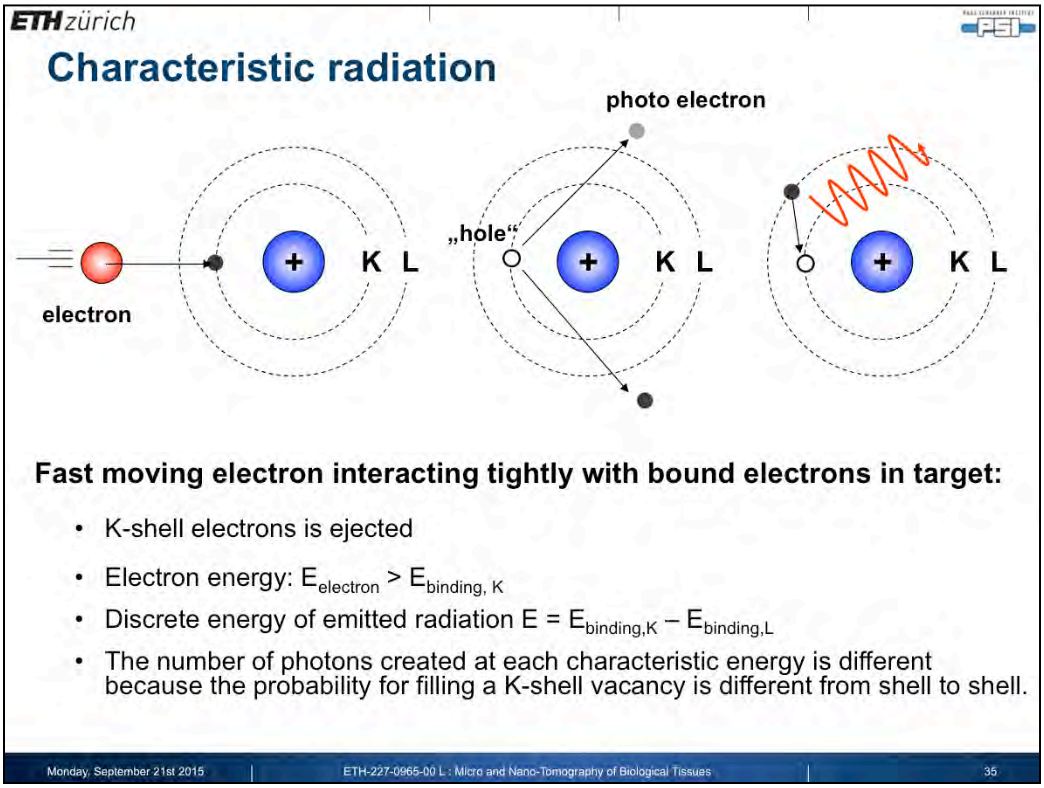

The type of interaction that produces **characteristic radiation**, involves a collision between the high-speed electrons and the orbital electrons in the atom. The interaction can occur only if the incoming electron has a kinetic energy greater than the **binding energy** of the electron within the atom. When this condition exists, and the collision occurs, the electron is dislodged from the atom. When the orbital electron is removed, it leaves a vacancy that is filled by an electron from a higher energy level. As the filling electron moves down to fill the vacancy, it gives up energy emitted in the form of an x-ray photon. This is known as characteristic radiation because the energy of the photon is characteristic of the chemical element that serves as the anode material.

Actually, a given anode material gives rise to several characteristic x-ray energies. This is because electrons at different energy levels (K, L, etc.) can be dislodged by the bombarding electrons, and the vacancies can be filled from different energy levels. The electronic energy levels in tungsten are shown below, along with some of the energy changes that give rise to characteristic photons. Although filling L-shell vacancies generates photons, their energies are too low for use in diagnostic imaging. Each characteristic energy is given a designation, which indicates the shell in which the vacancy occurred, with a subscript, which shows the origin of the filling electron. A subscript alpha denotes filling with an L-shell electron, and beta indicates filling from either the M or N shell

X-ray tube spectrum: characteristic radiation

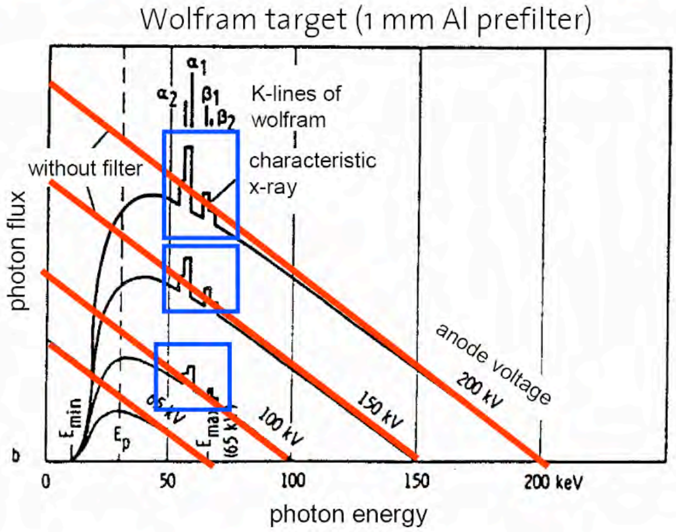

Bremsstrahlung → Continuous spectrum

Characteristic radiation → Peaks / Lines

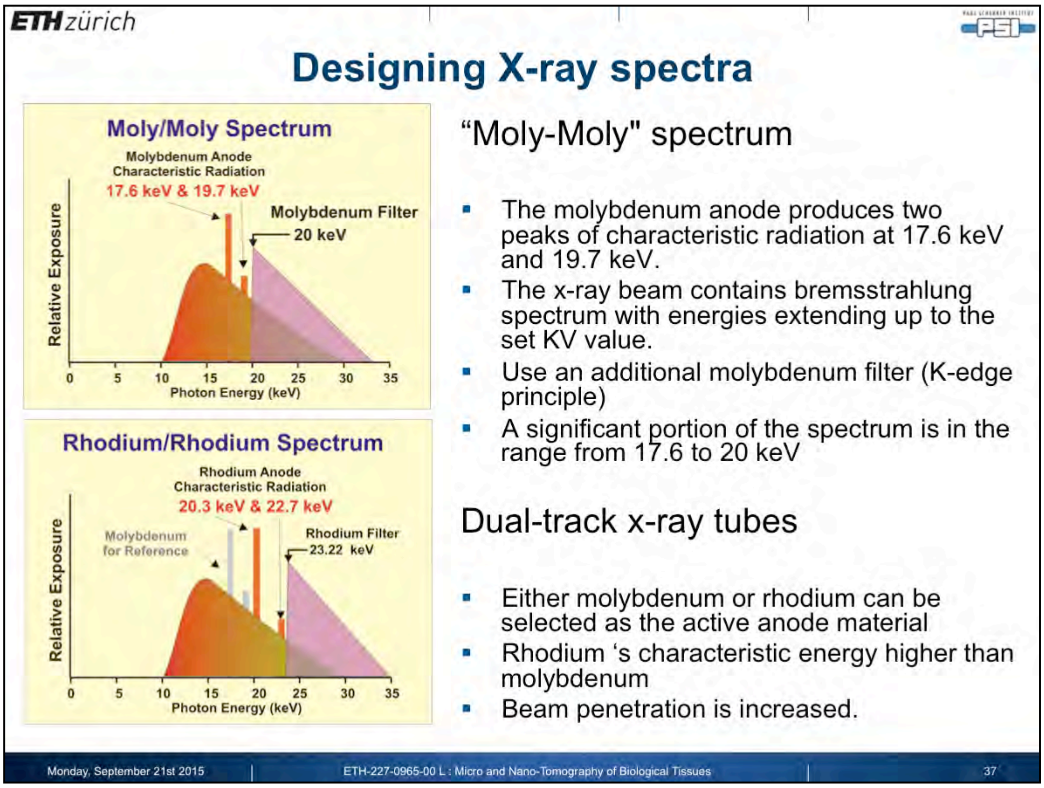

X-ray tube spectrum

The "moly-moly" spectrum is the most frequently used for mammography. The molybdenum anode produces two peaks of characteristic radiation at 17.6 keV and 19.7 keV as shown above. Let's notice that this is very close to the optimum spectrum, especially for the smaller and less dense breasts. However, the x-ray beam will also contain the usual bremsstrahlung spectrum with energies extending up to the set KV value which will be in the range of 24 kV to 32 kV. This part of the spectrum is undesirable because of its increased penetration which reduces the contrast. That problem is solved by using a molybdenum filter that works on the K-edge principle, that is it attenuates photons with energies above the molybdenum K edge energy of 20 keV.

With this combination a significant portion of the spectrum is in the range from 17.6 to 20 keV which is quite good for general mammography. With mammography equipment with only the "moly-moly" combination (the standard for many years) the only adjustable factor for changing the spectrum is the KV. As the KV is increased within the 24 - 32 kV range, the x-ray beam becomes more penetrating. Increasing the KV increases the amount (but not the photon energy) of the characteristic radiation and also increases the amount of bremsstrahlung just below the filter K edge cut-off.

Increasing the KV also increases the efficiency of x-ray production in the tube so that there is more radiation per MAS and per unit of heat. It is the combination of these factors (higher penetration and increased x-ray tube output) that makes the higher KV values necessary for larger and more dense breast, not only to achieve the necessary receptor exposure within a reasonable exposure time

Many mammography machines give the operator the opportunity of selecting between two filters, molybdenum or rhodium. Rhodium has a slightly higher atomic number (Z) that molybdenum and therefore its K-edge energy is higher, 23.22 keV. When the rhodium filter is selected the x-ray spectrum is now extended up to that energy and becomes more penetrating. The rhodium filter is useful when imaging dense breast where additional penetration improves visulation within the dense areas.

Some equipment have dual-track x-ray tubes so that either molybdenum or rhodium can be selected as the active anode material Because of its higher atomic number (Z) rhodium produces characteristic x-radiation with higher energies than molybdenum.

When the rhodium anode is selected (always with the rhodium filter) the beam penetration is increased and generally is optimum for imaging dense breast.

We have seen how the use of rhodium, both as a filter and anode material, extends the spectrum and makes it more penetrating. This does improve contrast and visibility in the more dense breast by making it possible to "see through" some of the dense areas. However, the increased penetration can reduce contrast in other breast environments.

X-ray interactions with matter

X-ray interactions with matter (relevant for microscopy)

- Terminology:
  - **Transmission:** photon passing through the body
  - **Absorption:** partial or total absorption of the photon energy
  - **Scatter:** photon deviated in a new direction
  - **Attenuation:** absorption + scatter

- Physical names:
  - Photo effect
  - Compton scattering
  - Pair-production

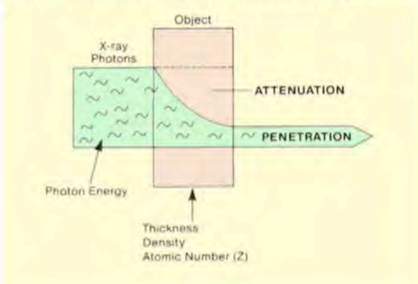

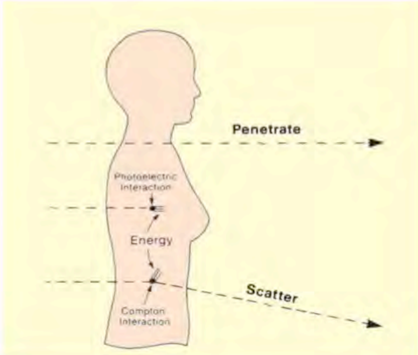

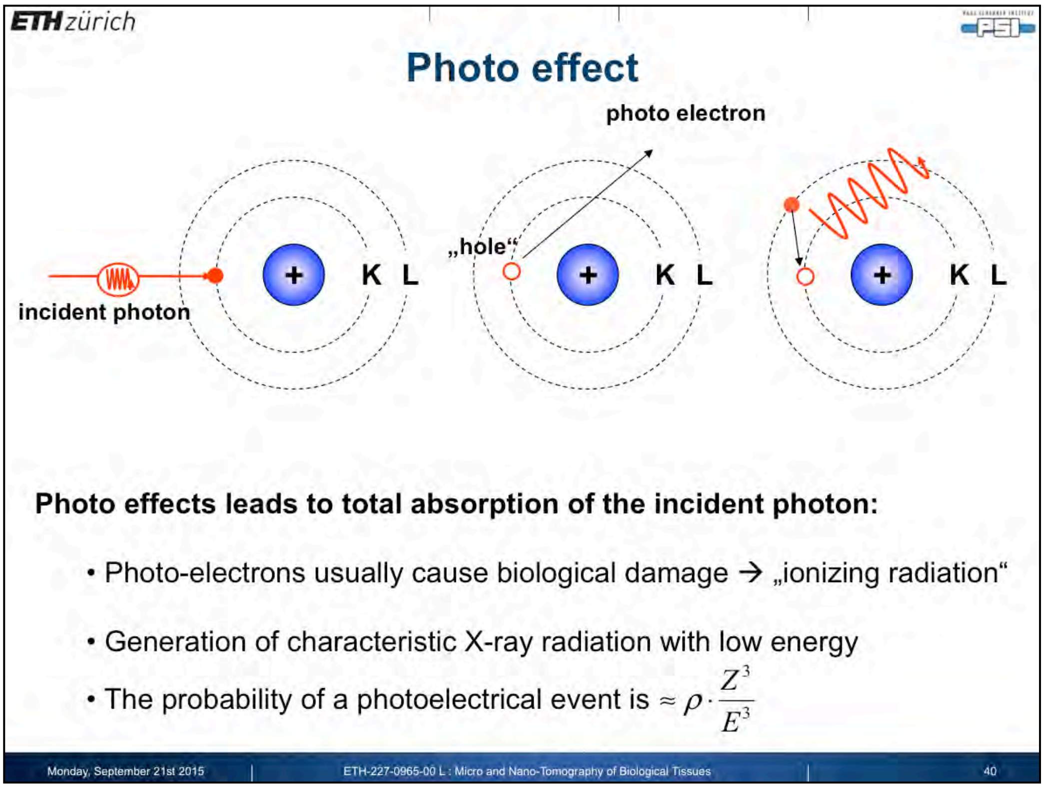

In the photoelectric (photon-electron) interaction, a photon transfers all its energy to an electron located in one of the atomic shells. The electron is ejected from the atom by this energy and begins to pass through the surrounding matter. The electron rapidly loses its energy and moves only a relatively short distance from its original location. The photon's energy is, therefore, deposited in the matter close to the site of the photoelectric interaction. The energy transfer is a two-step process. The photoelectric interaction in which the photon transfers its energy to the electron is the first step. The depositing of the energy in the surrounding matter by the electron is the second step.

Photoelectric interactions usually occur with electrons that are firmly bound to the atom, that is, those with a relatively high binding energy. Photoelectric interactions are most probable when the electron binding energy is only slightly less than the energy of the photon. If the binding energy is more than the energy of the photon, a photoelectric interaction cannot occur. This interaction is possible only when the photon has sufficient energy to overcome the binding energy and remove the electron from the atom.

The photon's energy is divided into two parts by the interaction. A portion of the energy is used to overcome the electron's binding energy and to remove it from the atom. The remaining energy is transferred to the electron as kinetic energy and is deposited near the interaction site. Since the interaction creates a vacancy in one of the electron shells, typically the K or L, an electron moves down to fill in. The drop in energy of the filling electron often produces a characteristic x-ray photon. The energy of the characteristic radiation depends on the binding energy of the electrons involved. Characteristic radiation initiated by an incoming photon is referred to as fluorescent radiation. Fluorescence, in general, is a process in which some of the energy of a photon is used to create a second photon of less energy. This process sometimes converts x-rays into light photons. Whether the fluorescent radiation is in the form of light or x-rays depends on the binding energy levels in the absorbing material

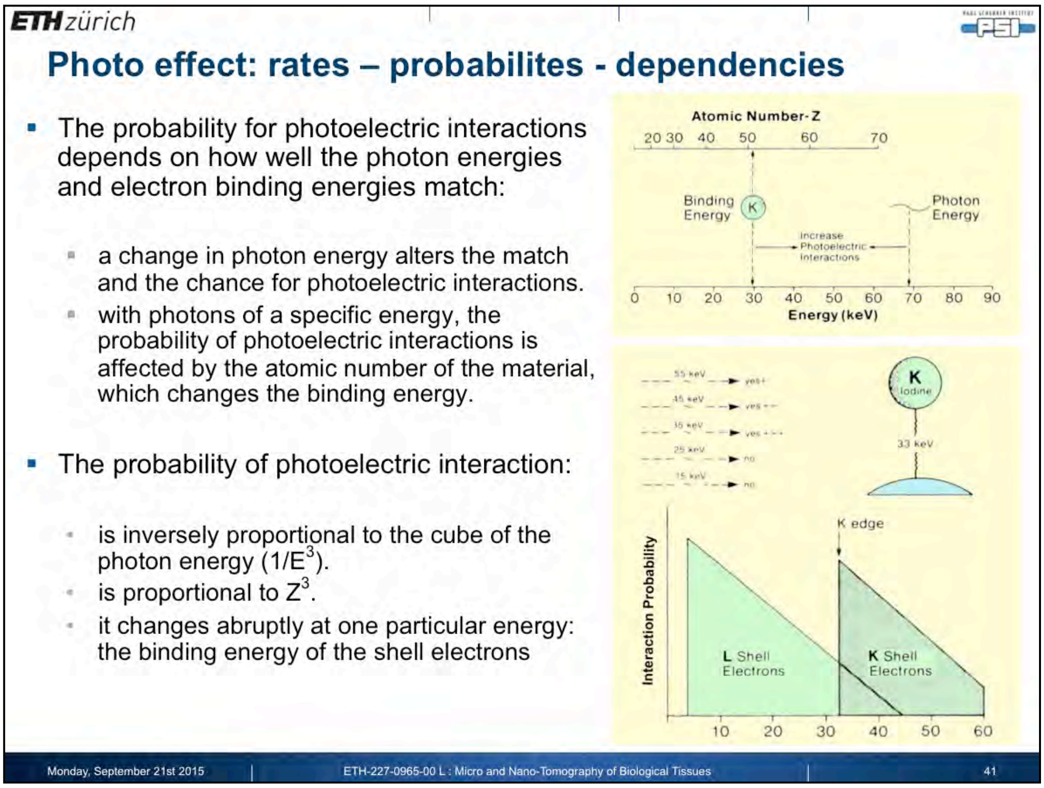

Photoelectric Rates

The probability, and thus attenuation coefficient value, for photoelectric interactions depends on how well the photon energies and electron binding energies match. This can be considered from two perspectives. In a specific material with a fixed binding energy, a change in photon energy alters the match and the chance for photoelectric interactions. On the other hand, with photons of a specific energy, the probability of photoelectric interactions is affected by the atomic number of the material, which changes the binding energy.

Dependence on Photon Energy

In a given material, the probability of photoelectric interactions occurring is strongly dependent on the energy of the photon and its relationship to the binding energy of the electrons. The slide shows the relationship between the attenuation coefficient for iodine (Z = 53) and photon energy. This graph shows two significant features of the relationship. One is that the coefficient value, or the probability of photoelectric interactions, decreases rapidly with increased photon energy. It is generally said that the probability of photoelectric interactions is inversely proportional to the cube of the photon energy (1/E3). This general relationship can be used to compare the photoelectric attenuation coefficients at two different photon energies. The significant point is that the probability of photoelectric interactions occurring in a given material drops drastically as the photon energy is increased.
The other important feature of the attenuation coefficient-photon energy relationship is that it changes abruptly at one particular energy: the binding energy of the shell electrons. The K-electron binding energy is 33 keV for iodine. This feature of the attenuation coefficient curve is generally designated as the K, L, or M edge. The reason for the sudden change is apparent if it is recalled that photons must have energies equal to or slightly greater than the binding energy of the electrons with which they interact. When photons with energies less than 33 keV pass through iodine, they interact primarily with the L-shell electrons. They do not have sufficient energy to eject electrons from the K shell, and the probability of interacting with the M and N shells is quite low because of the relatively large difference between the electron-binding and photon energies. However, photons with energies slightly greater than 33 keV can also interact with the K shell electrons. This means that there are now more electrons in the material that are available for interactions. This produces a sudden increase in the attenuation coefficient at the K-shell energy. In the case of iodine, the attenuation coefficient abruptly jumps from a value of 5.6 below the K edge to a value of 36, or increases by a factor of more than 6.
A similar change in the attenuation coefficient occurs at the L-shell electron binding energy. For most elements, however, this is below 10 keV and not within the useful portion of the x-ray spectrum.
Photoelectric interactions occur at the highest rate when the energy of the x-ray photon is just above the binding energy of the electrons.

Material Atomic Number

The probability of photoelectric interactions occurring is also dependent on the atomic number of the material. An explanation for the increase in photoelectric interactions with atomic number is that as atomic number is increased, the binding energies move closer to the photon energy. The general relationship is that the probability of photoelectric interactions (attenuation coefficient value) is proportional to Z3. In general, the conditions that increase the probability of photoelectric interactions are low photon energies and high-atomic-number materials.

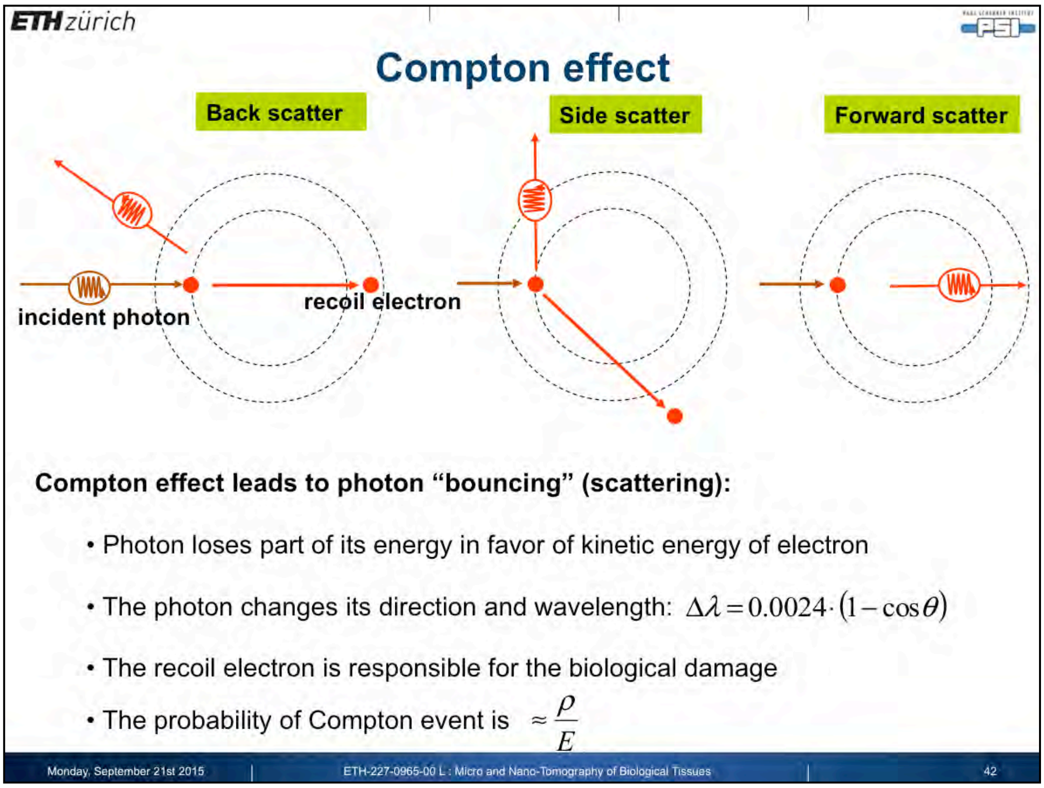

Compton interaction

A Compton interaction is one in which only a portion of the energy is absorbed and a photon is produced with reduced energy. This photon leaves the site of the interaction in a direction different from that of the original photon. Because of the change in photon direction, this type of interaction is classified as a scattering process. In effect, a portion of the incident radiation "bounces off' or is scattered by the material. This is significant in some situations because the material within the primary x-ray beam becomes a secondary radiation source. The most significant object producing scattered radiation in an x-ray procedure is the patient's body. The portion of the patient's body that is within the primary x-ray beam becomes the actual source of scattered radiation. This has two undesirable consequences. The scattered radiation that continues in the forward direction and reaches the image receptor decreases the quality (contrast) of the image; the radiation that is scattered from the patient is the predominant source of radiation exposure to the personnel conducting the examination.

Coherent Scatter

There are actually two types of interactions that produce scattered radiation. One type, referred to by a variety of names, including coherent, Thompson, Rayleigh, classical, and elastic, is a pure scattering interaction and deposits no energy in the material. Although this type of interaction is possible at low photon energies, it is generally not significant in most diagnostic procedures.

Energy of scattered radiation

When a photon undergoes a Compton interaction, its energy is divided between the scattered secondary photon and the electron with which it interacts. The electron's kinetic energy is quickly absorbed by the material along its path. In other words, in a Compton interaction, part of the original photon's energy is absorbed and part is converted into scattered radiation.
The manner in which the energy is divided between scattered and absorbed radiation depends on two factors-the angle of scatter and the energy of the original photon. The relationship between the energy of the scattered radiation and the angle of scatter is a little complex and should be considered in two steps. The photon characteristic that is specifically related to a given scatter angle is its change in wavelength. It should be recalled that a photon's wavelength (☒) and energy (**E**) are inversely related as given by:

E = 12.4 / ☒.

Since photons lose energy in a Compton interaction, the wavelength always increases. The relationship between the change in a photon's wavelength, ☒☒, and the angle of scatter is given by:

☒☒= 0.024 (1 - cos ☒).

For example, all photons scattered at an angle of 90 degrees, where the cosine has a value of 0, will undergo a wavelength change of 0.024 Å. Photons that scatter back at an angle of 180 degrees where the cosine has a value of -1 will undergo a wavelength change of 0.048 Å. This is the maximum wavelength change that can occur in a scattering interaction.

It is important to recognize the difference between a change in wavelength and a change in energy. Since higher energy photons have shorter wavelengths, a change of say 0.024 Å represents a larger energy change than it would for a lower energy photon. All photons scattered at an angle of 90 degrees will undergo a wavelength change of 0.0243Å The change in energy associated with 90-degree scatter is not the same for all photons and depends on their original energy. The change in energy can be found as follows. For a 110-keV photon, the wavelength is 0.1127 Å. A scatter angle of 90 degrees will always increase the wavelength by 0.0243. Therefore, the wavelength of the

Pair production

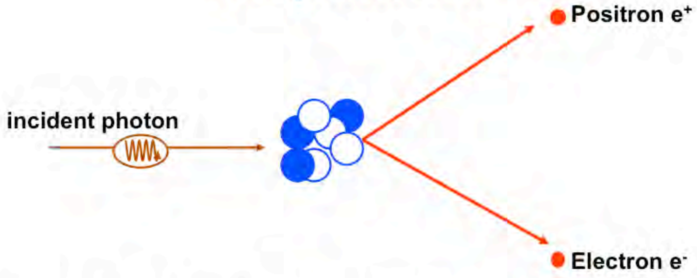

Incident photons (E > 1.02 MeV) may interact with a nucleus to form an electron-positron pair:

- Energy is just sufficient to provide the rest masses of the electron and positron (0.51 MeV each).
- Excess energy will be carried away equally by these two particles which produce ionisation as they travel in the material.
- The positron is eventually captured by an electron and annihilation of the two particles occurs.
- This results in the release of two photons each of 0.51 MeV known as annihilation radiation
- These two photons then lose energy by Compton scattering or photo effect.

Pair production is a photon-matter interaction that is not encountered in diagnostic procedures because it can occur only with photons with energies in excess of 1.02 MeV. In a pair-production interaction, the photon interacts with the nucleus in such a manner that its energy is converted into matter. The interaction produces a pair of particles, an electron and a positively charged positron. These two particles have the same mass, each equivalent to a rest mass energy of 0.51 MeV.

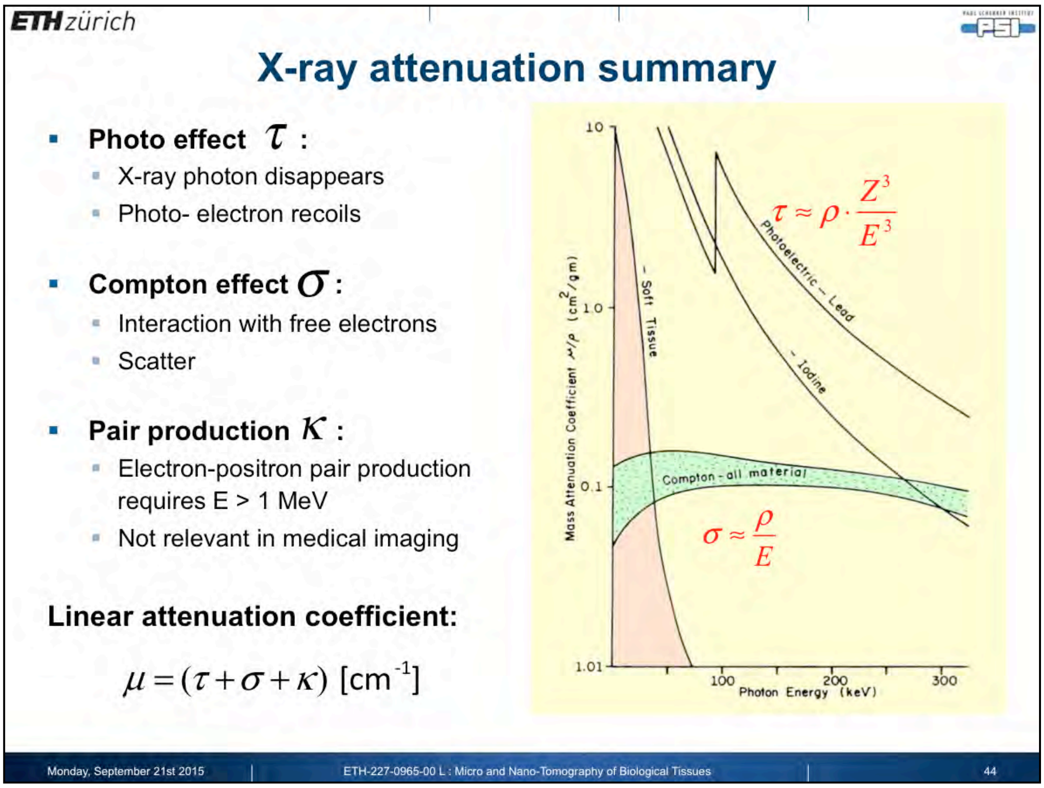

Competitive interactions

As photons pass through matter, they can engage in either photoelectric or Compton interactions with the material electrons. The photoelectric interaction captures all photon energy and deposits it within the material, whereas the Compton interaction removes only a portion of the energy, and the remainder continues as scattered radiation. The combination of the two types of interactions produces the overall attenuation of the x-ray beam. We now consider the factors that determine which of the two interactions is most likely to occur in a given situation.

The energy at which interactions change from predominantly photoelectric to Compton is a function of the atomic number of the material. The figure below shows this crossover energy for several different materials. At the lower photon energies, photoelectric interactions are much more predominant than Compton. Over most of the energy range, the probability of both decreases with increased energy. However, the decrease in photoelectric interactions is much greater. This is because the photoelectric rate changes in proportion to 1/E3, whereas Compton interactions are much less energy dependent. In soft tissue, the two lines cross at an energy of about 30 keV. At this energy, both photoelectric and Compton interactions occur in equal numbers. Below this energy, photoelectric interactions predominate. Above 30 keV, Compton interactions become the significant process of x-ray attenuation. As photon energy increases, two changes occur: The probability of both types of interactions decreases, but the decrease for Compton is less, and it becomes the predominant type of interaction.

In higher-atomic-number materials, photoelectric interactions are more probable, in general, and they predominate up to higher photon energy levels. The conditions that cause photoelectric interactions to predominate over Compton are the same conditions that enhance photoelectric interactions, that is, low photon energies and materials with high atomic numbers.

The total attenuation coefficient value for materials involved in x-ray and gamma interactions can vary tremendously if photoelectric interactions are involved. A minimum value of approximately 0.15 cm2/g is established by Compton interactions. Photoelectric interactions can cause the total attenuation to increase to very high values. For example, at 30 keV, lead (Z = 82) has a mass attenuation coefficient of 30 cm2/g.

Beer-Lambert's law

- Photons do not have the same range, even when they have the same energy.
- Some of the photons travel a relatively short distance before interacting, whereas others pass through or penetrate the object.
- The relationship between the number of photons reaching a specific point and the thickness of the material to that point is **exponential.**

- **Beer-Lambert's law:**

object dependence

$$I = I_0 \cdot e^{-\int_{0}^{\infty} \mu(x) \cdot dx}$$

$$I = \int_{0}^{E_{max}} I_0(E) \cdot e^{-\int_{-\infty}^{\infty} \mu(E,x) \cdot dx} \, dE$$

energy dependence

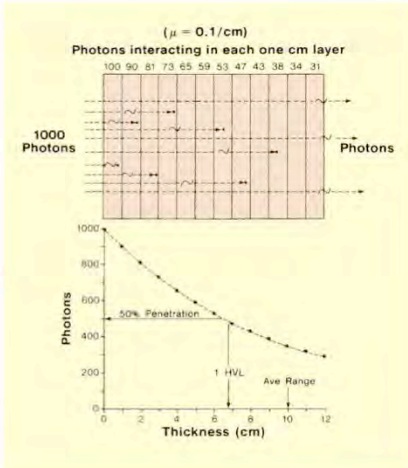

Beer-Lambert law: behind the curtains…

- Assume that particles may be described as having an absorption cross section (i.e. area), σ, perpendicular to the path of light through a solution, such that a X-ray photon is absorbed if it strikes the particle, and is transmitted if it does not.
- Define z as an axis parallel to the direction that X-ray photons are moving, and A and dz as the area and thickness (along the z axis) of a 3-dimensional slab of material through which light is passing. We assume that dz is sufficiently small that one particle in the slab cannot obscure another particle in the slab when viewed along the z direction. The concentration of particles in the slab is represented by N.
- It follows that the fraction of photons absorbed when passing through this slab is equal to the total opaque area of the particles in the slab, $\sigma\ A\ N\ dz$, divided by the area of the slab A, which yields $\sigma\ N\ dz$. Expressing the number of photons absorbed by the slab as dI_z, and the total number of photons incident on the slab as I_z, the fraction of photons absorbed by the slab is given by

$$\frac{dI_z}{I_z} = -\sigma \cdot N \cdot dz$$

- The solution to this simple differential equation is obtained by integrating both sides to obtain I_z as a function of z

$$\ln(I_z) = -\sigma \cdot N \cdot z + C$$

- The difference of intensity for a slab of real thickness ℓ is I_0 at $z = 0$, and I_l at $z = \ell$. Using the previous equation, the difference in intensity can be written as,

$$\ln(I_0) - \ln(I_l) = (-\sigma \cdot N \cdot 0 + C) - (-\sigma \cdot N \cdot l + C) = \sigma \cdot l \cdot N$$

- Which finally yields:

$$I_l = I_0 \cdot e^{-\sigma \cdot N \cdot l}$$

References

- **X-ray physics**
- Perry Sprawls, *The Physical Principles of Medical Imaging*, 2nd Ed
  http://www.sprawls.org/
- G. D. Boreman, *Modulation Transfer Function in Optical and Electro-Optical Systems,* SPIE, Bellingham, WA, ISBN 0-8194-4143-0

- **Computed tomography:**
- A. C. Kak, M. Slaney, Principle of Computerized Tomographic Imaging", SIAM Classics in Applied Mathematics 33, New York, 2001, ISBN 0-89871-494-X
- F. Natterer, *"The Mathematics of Computerized Tomography",* SIAM Classics in Applied Mathematics 32, Philadelphia 2001, ISBN 0-89871-493-1
- W. A. Kalender, *"Computed Tomography – Fundamentals, System Technology, Image Quality, Applications",* 2nd revised edition, 2005, Publicis Corporate Publishing, ISBN 3-89578-216-5
- J. Hsieh, *Computed Tomography: Principles, Design, Artifacts and Recent Advances,* SPIE Press Monograph, ISBN 0-8194-4425-1

Appendix I

Appendix Ia: Linear/mass attenuation coefficient

Linear attenuation coefficient:

$$\mu = \mu' \cdot \rho \ [\mathrm{cm}^{-1}]$$

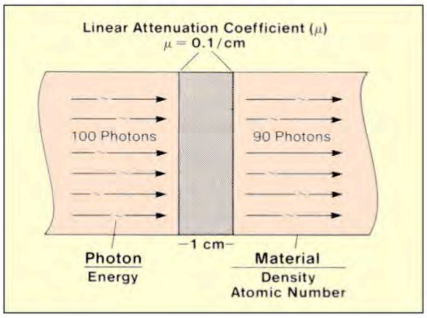

Mass absorption coefficient:

$$\mu' [\mathrm{cm}^2/\mathrm{g}]$$

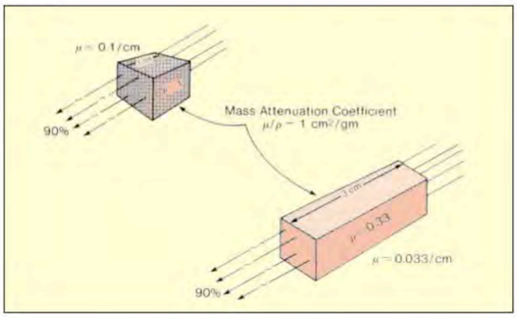

Linear Attenuation Coefficient

As a photon makes its way through matter, there is no way to predict precisely either how far it will travel before engaging in an interaction or the type of interaction it will engage in. In clinical applications we are generally not concerned with the fate of an individual photon but rather with the collective interaction of the large number of photons. In most instances we are interested in the overall rate at which photons interact as they make their way through a specific material.
Let us observe what happens when a group of photons encounters a slice of material that is 1 unit thick, as illustrated in slide. Some of the photons interact with the material, and some pass on through. The interactions, either photoelectric or Compton, remove some of the photons from the beam in a process known as attenuation. Under specific conditions, a certain percentage of the photons will interact, or be attenuated, in a 1-unit thickness of material. The Linear attenuation coefficient (μ) is the actual fraction of photons interacting per 1-unit thickness of material. In our example the fraction that interacts in the 1-cm thickness is 0.1, or 10%, and the value of the linear attenuation coefficient is 0.1 per cm.
Linear attenuation coefficient values indicate the rate at which photons interact as they move through material and are inversely related to the average distance photons travel before interacting. The rate at which photons interact (attenuation coefficient value) is determined by the energy of the individual photons and the atomic number and density of the material.

Mass Attenuation Coefficient

In some situations it is more desirable to express the attenuation rate in terms of the mass of the material encountered by the photons rather than in terms of distance. The quantity that affects attenuation rate is not the total mass of an object but rather the area mass. Area mass is the amount of material behind a 1-unit surface area, as shown below. The **area mass** is the product of material thickness and **density**:

Area Mass (g/cm2) = Thickness (cm) x Density (g/cm3).

The mass attenuation coefficient is the rate of photon interactions per 1-unit (g/cm2) area mass.
The figure compares two pieces of material with different thicknesses and densities but the same area mass. Since both attenuate the same fraction of photons, the mass attenuation coefficient is the same for the two materials. They do not have the same linear attenuation coefficient values.

The relationship between the mass and linear attenuation coefficients is

Mass Attenuation Coefficient (μ/r) = Linear Attenuation Coefficient (μ) / Density (r).

Notice that the symbol for mass attenuation coefficient (μ/r) is derived from the symbols for the linear attenuation coefficient (μ) and the symbol for density (r). We must be careful not to be misled by the relationship stated in this manner. Confusion often arises as to the effect of material density on attenuation coefficient values. Mass attenuation coefficient values are actually normalized with respect to material density, and therefore do not change with changes in density. Material density does have a direct effect on linear attenuation coefficient values.

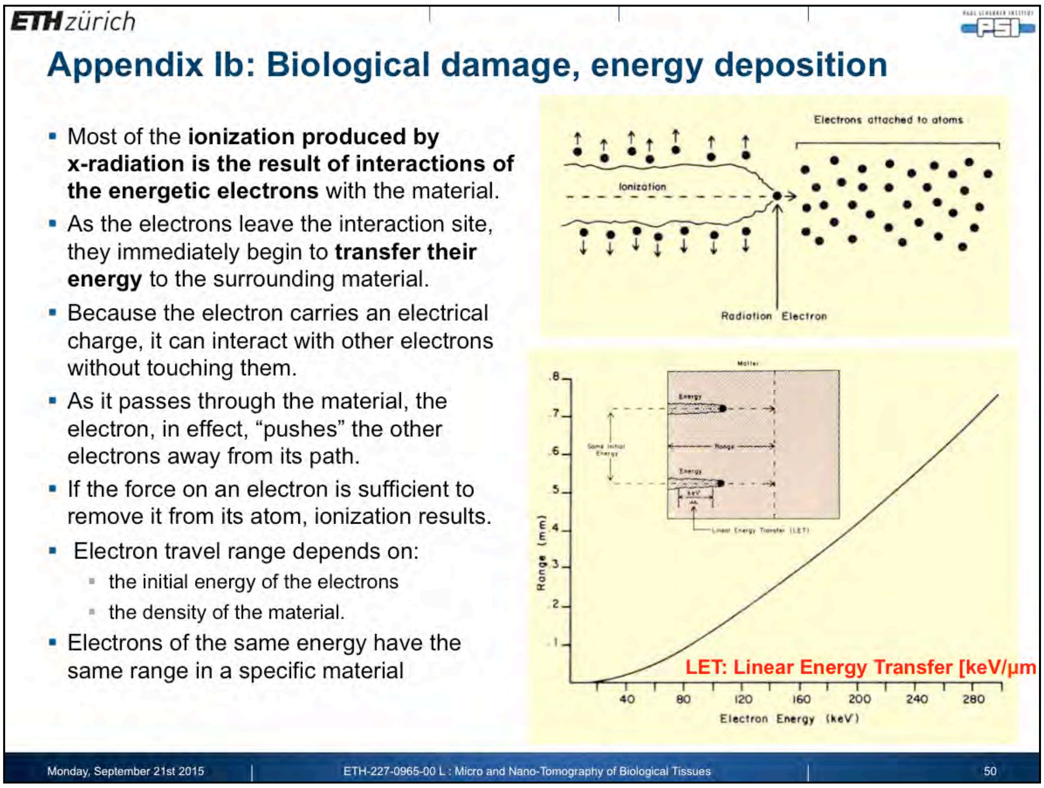

As the electrons leave the interaction site, they immediately begin to transfer their energy to the surrounding material. Because the electron carries an electrical charge, it can interact with other electrons without touching them. As it passes through the material, the electron, in effect, pushes the other electrons away from its path. If the force on an electron is sufficient to remove it from its atom, ionization results. In some cases, the atomic or molecular structures are raised to a higher energy level, or excited state. Regardless of the type of interaction, the moving electron loses some of its energy. Most of the ionization produced by x- and gamma radiation is not a result of direct photon interactions, but rather of interactions of the energetic electrons with the material. For example, in air, radiation must expend an average energy of 33.4 eV per ionization. Consider a 50-keV x-ray photon undergoing a photoelectric interaction. The initial interaction of the photon ionizes one atom, but the resulting energetic electron ionizes approximately 1,500 additional atoms

The total distance an electron travels in a material before losing all its energy is generally referred to as its range. The two factors that determine the range are (1) the initial energy of the electrons and (2) the density of the material. One important characteristic of electron interactions is that all electrons of the same energy have the same range in a specific material. The general relationship between electron range and energy is shown in the slide. The curve shows the range for a material with a density of 1 g/cm3. This is the density of water and the approximate density of muscle tissue.

LET

The rate at which an electron transfers energy to a material is known as the linear energy transfer (LET), and is expressed in terms of the amount of energy transferred per unit of distance traveled. Typical units are kiloelectron volts per micrometer (keV/um). In a given material, such as tissue, the LET value depends on the kinetic energy (velocity) of the electron. The LET is generally inversely related to the electron velocity. As a radiation electron loses energy, its velocity decreases, and the value of the LET increases until all its energy is dissipated.

The effectiveness of a particular radiation in producing biological damage is often related to the LET of the radiation. The actual relationship of the efficiency in producing damage to LET values depends on the biological effect considered. For some effects, the efficiency increases with an increase in LET, for some it decreases, and for others it increases up to a point and then decreases with additional increases in LET. For a given biological effect, there is an LET value that produces an optimum energy concentration within the tissue. Radiation with lower LET values does not produce an adequate concentration of energy. Radiations with higher LET values tend to deposit more energy than is needed to produce the effect; this tends to waste energy and decrease efficiency.

Abell 1689: A galaxy cluster at a distance of about 2.3 billion light years from Earth.

This image of Abell 1689 is a composite of data from the Chandra X-ray Observatory (purple) and the Hubble Space Telescope (yellow). Abell 1689 is a massive cluster of galaxies that shows signs of merging activity. The long arcs in the optical image, the largest system of such arcs ever found, are caused by gravitational lensing of the background galaxies by matter in the galaxy cluster. Further studies of this cluster are needed to explain the lack of agreement between mass estimates based on the X-ray data and on the gravitational lensing.

Scale: Image is 3.2 arcmin across.

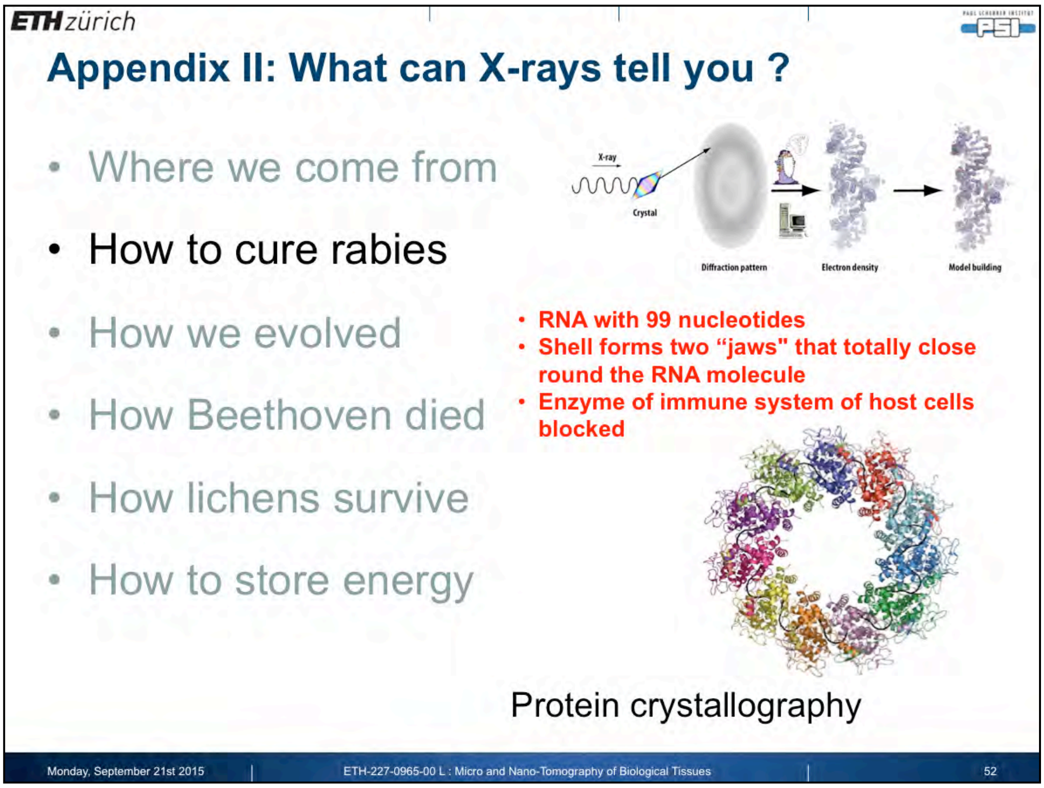

Protein Cristallography

X-ray crystallography is a method of determining the arrangement of atoms within a crystal, in which a beam of X-rays strikes a crystal and causes the beam of light to spread into many specific directions. From the angles and intensities of these diffracted beams, a crystallographer can produce a three-dimensional picture of the density of electrons within the crystal. From this electron density, the mean positions of the atoms in the crystal can be determined, as well as their chemical bonds, their disorder and various other information.

Cracking the rabies virus protection shield

Louis Pasteur developed the first effective vaccine against rabies more than 100 years ago, by growing the virus in rabbits, and then weakening it by drying the affected nerve tissue.

Nowadays, there are very efficient vaccines. However, in poorer countries where public health care is absent, rabies in humans is still common, accounting for over 50 000 deaths per year. The vaccine needs to be kept constantly refrigerated for it to work effectively. Rabies, like some other pernicious forms of viruses, including ebola and measles, is unusual in that in order for it to be able to infect a host cell, its RNA (ribonucleic acid) must first be transcribed into messenger-RNA, which then codes for the viral protein, allowing the virus to reproduce. For this first transcription step, the virus's RNA must be encapsulated in a large and complicated protein-RNA complex, known as a nucleocapsid, or protein shell. In a joint effort, groups from the Universite Joseph Fourier-CNRS and the European Molecular Biology Laboratory in Grenoble were able to produce a recombinant system of the viral RNA and its shell. The RNA molecule is very short, consisting of only 99 nucleotides (i.e., RNA building blocks), and the nucleoprotein molecules at each end attract one another chemically so that a circular structure is formed. This was successfully crystallized, and the orthorhombic structure was recorded down to a resolution of 3.5 AA. By isomorphous replacement, 2 rings of 11 gold atoms were inserted into each complex, and a second set of x-ray diffraction data was recorded down to a resolution of 6 A at the Au L-III edge at a wavelength of 1.0372 A.

It was seen that the shell consists of 11 groups known as “protomers", each group binding to 9 nucleotides. Crucially, the nucleoprotein shell forms two “jaws" that totally close round the RNA molecule, rendering it inaccessible to outside chemicals such as enzymes. The shell therefore acts as a protecting shield, which is able to distinguish between dierent types of enzymes trying to gain access to the RNA coil (those enzymes from the immune system of the host cell, which attempt to degrade and destroy the foreign RNA, are blocked, while in an environment where the RNA virus can replicate, the jaw mechanism is opened).

This structure and mechanism suggests two ways in which the rabies virus might be neutralized. The first would be to lock the hinge of the jaws, so that replication is always inhibited. The other would be to force the jaw open at a time when the internal RNA can be attacked by the immune system enzymes. Hence, the final goal is to design cheap and effective drugs which are able to combat rabies in poor countries.

XTM: the spread of hominoids

The evolution of the hominoids (the great apes) counts as one of the most controversial and emotive debates in the natural sciences. Although it is generally agreed that the first hominoids lived around 20 million years (MY) ago, at the start of the miocene period, their subsequent spread and diversification is still disputed. It is known that the first examples of species found outside Africa date to some 16:5 MY ago, and between 12 and 6 MY ago (the end of the miocene period), many different forms are known to have existed in Africa, Asia, and Europe. Diversification seems to have declined since then, probably as a result of climate changes, and now, only five genera, the gibbons, orangutans, gorillas, chimpanzees, and man, remain. Conventional theory has it that the principal area of diversification was in Africa during the whole of the Miocene period, with succesive migrations to Europe and Asia, and local evolution on all three continents (see Fig. 9.5). In an alternative hypothesis, however, it is suggested that, primitive forms of hominoids migrated from Africa and that most of the diversification happened in Asia, while the original species became extinct in Africa. Only later, it is proposed, was Africa repopulated and migration to Europe occurred. Fossil records from both Africa and Asia should, therefore, provide valuable evidence to test these competing theories. In 2003, a previously unknown species of hominoid was discovered in Thailand, dating from approximately 12 MY ago. The fossil record consisted of about 20 isolated teeth1 attributed to several male and female individuals. The large differences in their sizes showed that this species was large, with a strong sexual dimorphism, i.e., the

male was much larger than the female, This new species was christened Lufengpithecus chiangmuanensis. Although traditional palaeontological studies of the external dental morphology provide valuable information, the internal structure of the teeth is equally important. Normally, this can only be gleaned by cutting through the teeth, thereby destroying it.

XTM allows one, however, to probe the internal structure in a nondestructive way. In this manner, it was possible to quantify precisely the thickness and distribution of the dental enamel. Surprisingly, it was found that this fossil species is more similar to modern orangutans than to any other known fossil hominoids found in Asia. It was therefore tentatively proposed that Lufengpithecus chiangmuanensis might be a direct ancestor of modern day orangutans. The plot thickened, however, the following year in 2004, when a complete mandible (lower jawbone), approximately 7 MY old, was discovered, also in Thailand, and was assigned to yet another new species, named Khoratpithecus piriyai (Khorat is the region in Thailand where the fossils were discovered). From traditional palaeontological methods, it seemed clear that these two fossils were more similar to one another than to any other fossil or living species, despite the fact that one fossil was older than the other by some 5 MY. This older fossil was consequently renamed Khoratpithecus chiangmuanensis. K. piriyai's mandible was also imaged at the European Synchrotron Research Facility (ESRF) using XTM, resulting in the first high-quality scan of such a large fossil of a hominoid. Using this exceptional data set, it was possible to analyse the dental structure and the bone architecture, and to virtually extract the teeth from the right side of the mandible to study the size and the shape of tooth roots. The XTM data of K. chiangmuanensis's teeth were then used in a virtual reconstruction of its jaws. This allowed further comparisons of the reconstructed jaws of the older species and the surviving mandible of the younger fossil, including the relative sizes of teeth in the two species of Khoratpithecus. This showed that their similarities were even stronger than at first believed and strengthen the justification of their classification in a single genus, made on the basis of traditional palaeontological studies. Using XTM imaging of these fossils, it was therefore possible to reveal anatomical characteristics that would otherwise have been impossible to study without destroying the fossils. Hence, along with traditional methods, XTM revealed that Khorapithecus is the known genus most closely related to the orangutans, although specialized features in the more modern K. piriyai are very unlike modern orangutans. From what is generally known from other lineages, it therefore seems unlikely that so many specializations would have evolved and subsequently disappeared and hence K. piriyai is probably a distant cousin to modern orangutans rather than being a direct ancestor. The older species K. chiangmuanensis, however, shows fewer specialized dental characteristics, and is therefore a more likely candidate for being a direct ancestor of the orangutans. More fossil discoveries are necessary to test the hypothesis, but it remains very possible that the orangutan's lineage was derived from primitive forms of Khoratpithecus and that the two branches evolved in different ways, giving rise both to the orang-utans and to later species of Khoratpithecus, such as K. piriyai. We now return to our two hypotheses of hominoid evolution: African and Asian diversification. The two Khoratpithecus species, as well as the numerous other fossil hominoids from Asia, show a higher diversity than African hominoid fossils during the same period. Moreover, both very specialized and primitive species have been found in Asia. Together, the high levels of diversity and the wide geographic distribution in geological strata of Asian hominoids (from 16:5 MY ago to the present) strongly suggest that Asia was an important, perhaps even the principal, centre of diversification for Miocene hominoids. Increasingly, therefore, modern palaeological research is lending weight to the newer hypothesis of hominoid evolution: our hominoid ancestors originated in Africa, after which they diversied in Asia and repopulated Africa and Europe.

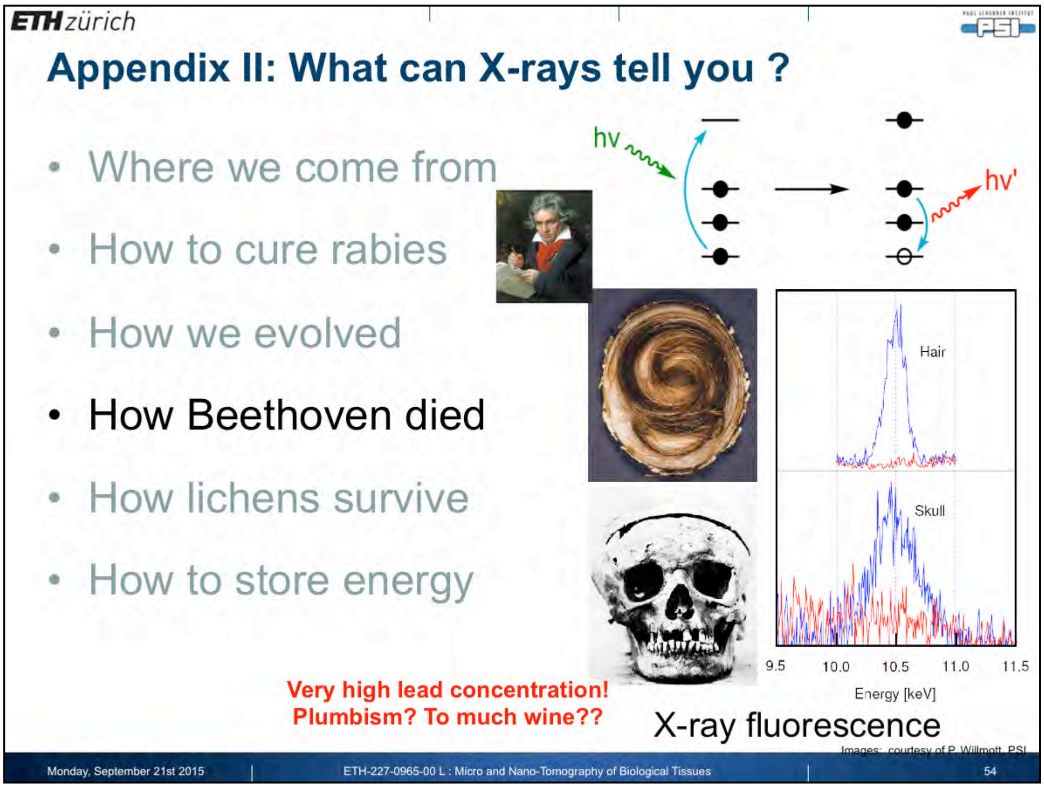

X-ray Fluorescence Spectroscopy

When materials are exposed to short-wavelength X-rays or to gamma rays, ionisation of their component atoms may take place. Ionisation consists of the ejection of one or more electrons from the atom, and may occur if the atom is exposed to radiation with an energy greater than its ionisation potential. X-rays and gamma rays can be energetic enough to expel tightly held electrons from the inner orbitals of the atom. The removal of an electron in this way renders the electronic structure of the atom unstable, and electrons in higher orbitals "fall" into the lower orbital to fill the hole left behind. In falling, energy is released in the form of a photon, the energy of which is equal to the energy difference of the two orbitals involved. Thus, the material emits radiation, which has energy characteristic of the atoms present. The term *fluorescence* is applied to phenomena in which the absorption of radiation of a specific energy results in the re-emission of radiation of a different energy (generally lower).

Beethoven's heavy metal

Ludwig van Beethoven suffered decades of illness in his adult life, including chronic indigestion, abdominal pains, irritability, and depression. Many possible causes have been suggested, including syphilis, which, at the turn of the 19th century, was commonly treated with mercury compounds. The days after Beethoven's death, a young musician named Ferdinand Hiller cut a large lock of the composer's hair as a keepsake. Over the intervening century and a half, the lock changed ownership until four americans, associated with societies dedicated to the history and works of the great composer, purchased it at a Sotheby's auction. They decided to allow the lock to be used in non-destructive chemical tests to help clarify any chemical (i.e., poisonous) cause of Beethoven's suffering.

In addition, Beethoven's remains were exhumed in 1863, and fragments of the skull were given to Dr. Romeo Seligmann, and remained in the family through four generations.

In 1999, the present generation, Paul and Joan Kaufmann, allowed the Advanced Photon Source (APS) at the Argonne National Laboratories, Illinois, to study the bone fragments..

Although no evidence for mercury poisoning could be identified (thereby weakening the hypothesis that Beethoven suffered and died from tertiary syphilis), concentrations of lead some hundred times larger than those found in healthy subjects were identified. The bone results are particularly significant, as such high concentrations of lead could only have accumulated after a prolonged exposure to lead. The origin of Beethoven's plumbism, however, remains unclear. Although he was known to be a connoisseur of wines, which at that time contained high levels of lead,

and was exposed to other potential sources of lead, there is little convincing evidence his was an exceptional case. It may simply be that he was hypersensitive to lead and his body may not have been able to eliminate it. Interestingly, plumbism does not normally result in deafness, and hence the composer's most famous ailment appears less likely to have been related to lead poisoning.

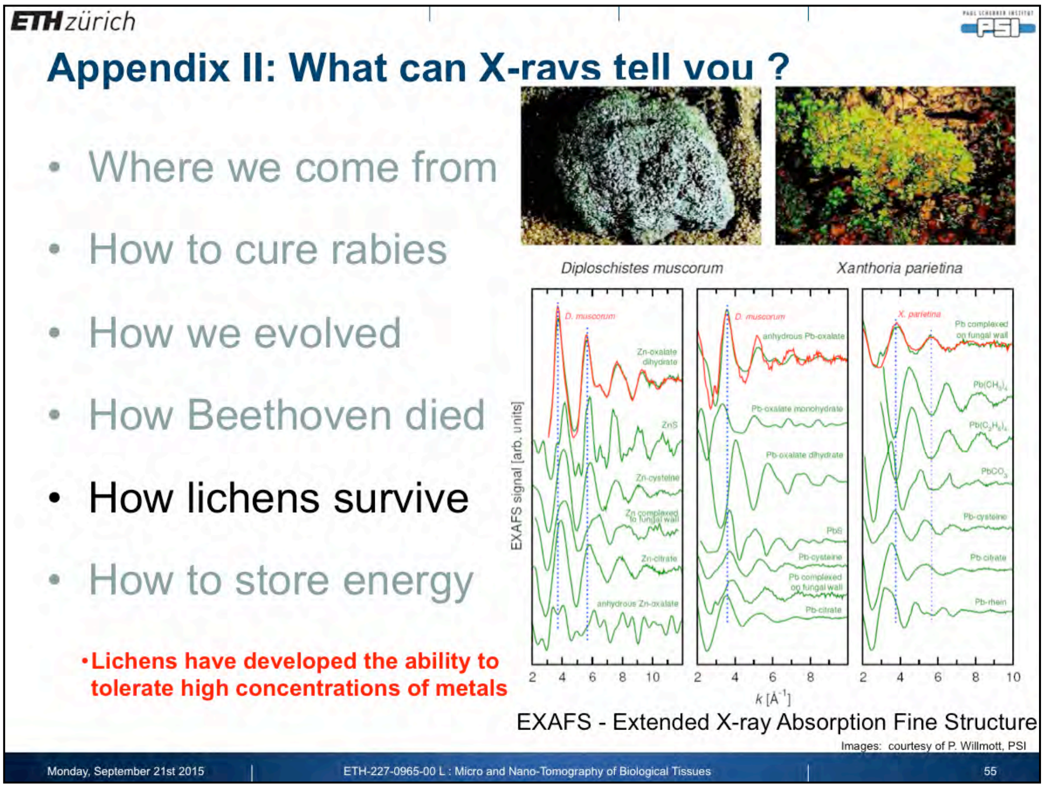

EXAFS:

X-ray Absorption Spectroscopy (XAS) includes both Extended X-Ray Absorption Fine Structure (EXAFS) and X-ray Absorption Near Edge Structure (XANES). XAS is the measurement of the x-ray absorption coefficient of a material as a function of energy. X-rays of a narrow energy resolution are shone on the sample and the incident and transmitted x-ray intensity is recorded as the incident x-ray energy is incremented.

Resistance of lichens to metallic pollution

Some lichens have developed the ability to tolerate high concentrations of metals and thereby prosper in heavily contaminated areas unsuitable to other plant species. The biochemical mechanisms responsible for this resilience are largely unknown. It can be shown how its high sensitivity down to around 100 mg/kg and the fact that metals in plants and lichen tend to be bound to functional groups of biological molecules, which are generally uncrystallized or only poorly crystallized, makes EXAFS ideally suited to investigate such protective adaptations.

Two species of lichen were investigated by G. Sarret et al.: Diploschistes muscorum, harvested in the vicinity of a zinc and lead smelter in northern France, and Xanthoria parietina, sampled on cement poles near a tetraethyl and tetramethyl lead factory near Nantes, France. It is known that metals collect as inactive complexes of carboxylic groups on the fungal walls of Penicillin chrysogenum, which has a very similar cell wall structure to D. muscorum and X. parietina. It was therefore thought that the two lichens under investigation might use the same mechanism, and so a sample of P. chrysogenum was contaminated with Zn and Pb, and used as a reference check.

EXAFS experiments were carried out at the Zn K edge for D. muscorum and at the Pb LIII edge for both lichen species. Comparing several potential binding complexes and mechanisms of Zn and Pb allowed the authors to conclude that in D. muscorum, Pb and Zn are accumulated through an enhanced oxalate synthesis, which precipitates toxic elements as insoluble salts. X. parietina, on the other hand, complexed Pb to carboxylic groups of the fungal wall cells in the same manner as does P. chrysogenum.

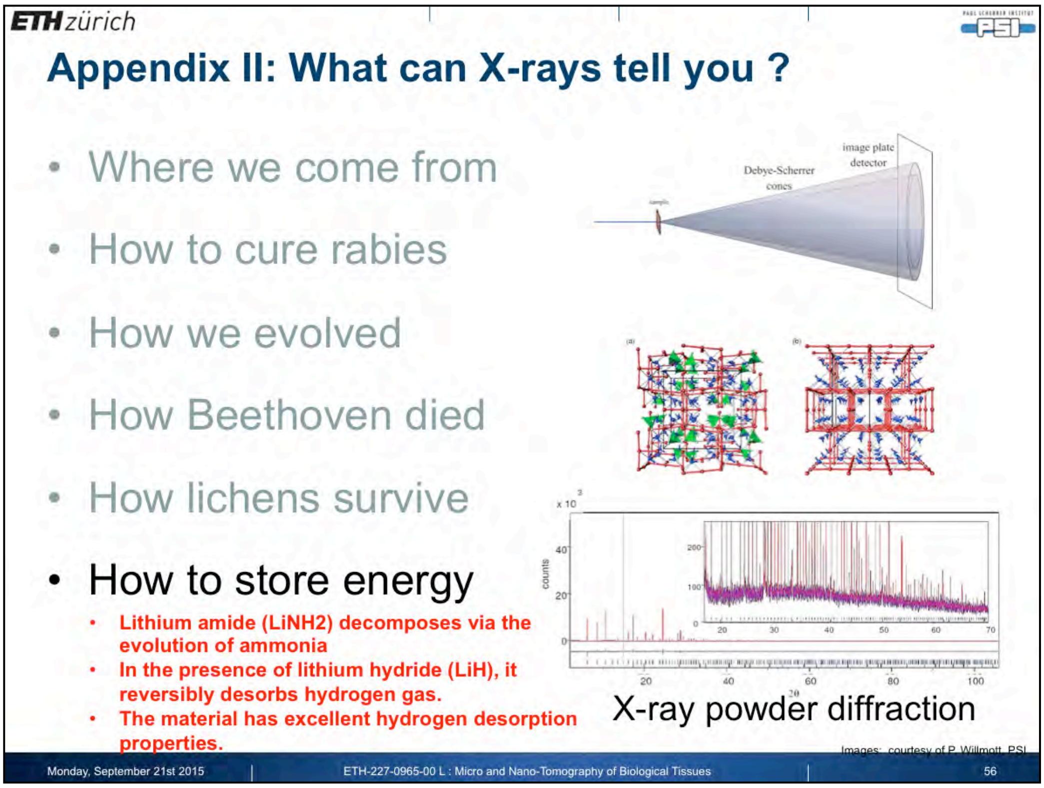

Powder diffraction

Ideally, every possible crystalline orientation is represented very equally in a powdered sample. The resulting orientational averaging causes the three-dimensional reciprocal space that is studied in single crystal diffraction to be projected onto a single dimension. The three-dimensional space can be described with (reciprocal) axes x*, y* and z* or alternatively in spherical coordinates q, φ*, and χ*. In powder diffraction, intensity is homogeneous over φ* and χ*, and only q remains as an important measurable quantity. In practice, it is sometimes necessary to rotate the sample orientation to eliminate the effects of texturing and achieve true randomness.

When the scattered radiation is collected on a flat plate detector, the rotational averaging leads to smooth diffraction rings around the beam axis, rather than the discrete Laue spots observed in single crystal diffraction. The angle between the beam axis and the ring is called the *scattering angle* and in X-ray crystallography always denoted as 2θ. (In scattering of *visible* light the convention is usually to call it θ).

Powder diffraction data are usually presented as a *diffractogram* in which the diffracted intensity I is shown as function either of the scattering angle 2θ or as a function of the scattering vector q. The latter variable has the advantage that the diffractogram no longer depends on the value of the wavelength λ. The advent of synchrotron sources has widened the choice of wavelength considerably. To facilitate comparability of data obtained with different wavelengths the use of q is therefore recommended and gaining acceptability. An instrument dedicated to perform powder measurements is called a powder diffractometer.

Solid-state hydrogen storage

Hydrogen is presently the most promising alternative to carbon-based fuels: it can be produced from a variety of renewable resources, and - when incorporated in fuel cells - offers near-zero emissions of pollutants and greenhouse gases. The development of a viable solid-state storage material is one of the primary